Mechanism and Machine Theory 169 (2022) 104636

Contents lists available at ScienceDirect

Mechanism and Machine Theory

journal homepage: www.elsevier.com/locate/mechmt

Repelling-screw-based geometrical interpretation of dualities of compliant mechanisms

Kun Wang [a,1], Huixu Dong [b,1], Chen Qiu [a,c,*], I-Ming Chen [b], Jian S. Dai [a]

[a] Centre for Robotics Research, King's College London, London WC2R 2LS, United Kingdom
[b] Robotics Research Centre, Nanyang Technological University, 50 Nanyang Avenue, Singapore
[c] Maider Medical Industry Equipment Co., Ltd

ARTICLE INFO

Keywords:
Compliant mechanisms
Repelling screw
Duality
Configuration transformation
Geometrical interpretation

ABSTRACT

This paper provides a geometrical insight into the dualities of compliant mechanisms via repelling screws. A method for the construction of the repelling screw system is proposed. By means of screw theory and linear algebra, the closed-loop relationships among the twist/wrench spaces of both actuation- and constraint-screw systems are identified, upon which the kinematics, statics and stiffness/compliance of both full- and limited-mobility compliant mechanisms are analysed. The internal correlations between repelling screws and dualities of mechanisms are investigated, which reveals both orthogonal and dual properties of mechanisms with either parallel or serial configuration. The repelling-screw-based representation is applied to describing the permitted motions and restricted constraints of the mechanism. In addition, a novel and systematic approach for parallel-to-serial/serial-to-parallel transformation is proposed, which retains the capability of changing the constraints and relative dimensions of the target configuration to better suit a specific task. A few examples conducted demonstrate the feasibility of the proposed approach and the effectiveness of the repelling-screw based interpretations of mechanism geometries.

1. Introduction

Compliant mechanism design plays a pivotal role in enabling robots to work in practical scenarios [1–4]. The behaviors based on compliant mechanisms can be modeled through elastic serial or parallel mechanisms, which provides a theoretical base for what alternative designs to be considered for completing some tasks. Apart from the theoretical constructions, many efforts have been made to developing compliant robotic systems for practical applications, including but not limited to, confined-space surgical applications [5], nano-manipulators [6], sensors [7], as well as compliant robotic grippers [8]. In addition, analytical approaches based on the compliant serial or parallel mechanism for modeling robot's kinematics and stiffness have been extended to evaluate novel designs with various materials, configurations, and actuation systems [9–11].

The demand for a compliant system leads to the study of elastic behaviors. Using screw theory [12], Dimentberg [13] studied the static and small vibrations of rigid platforms suspended by line springs. Lončarić [14] analysed the synthesis problem of stiffness matrix using Lie groups. Huang and Schimmels [15–17] systematically investigated the decomposition and realization of spatial

* Corresponding author.
E-mail address: chen.qiu@maiderchina.com (C. Qiu).
[1] These authors contributed equally to this work.

https://doi.org/10.1016/j.mechmachtheory.2021.104636
Received 22 August 2021; Received in revised form 18 October 2021; Accepted 3 November 2021
Available online 3 December 2021

Nomenclature

Symbols	descriptions
$\boldsymbol{S}$	plücker ray coordinated screw
$\boldsymbol{S}_{axis}$	plücker axis coordinated screw
Δ	the elliptical polar operator
$\boldsymbol{s}$	the axis vector of a screw
$\boldsymbol{r}$	the distance vector between the origin O and an axis vector $\boldsymbol{s}$
$\mathbb{S}$	screw system
$\mathbb{S}_r$	repelling screw system
$\mathbf{Ad}$	the adjoint transformation matrix
$\mathbb{T}_s$	the twist space of springs
$\mathbf{T}_s$	the basis of $\mathbb{T}_s$
$\boldsymbol{S}_t$	the element of $\mathbb{T}_s$
$\mathbb{W}_s$	the wrench space of springs
$\mathbf{W}_s$	the basis of $\mathbb{W}_s$
$\boldsymbol{S}_w$	the element of $\mathbb{W}_s$
$\mathbb{T}_c$	the twist space of constraints
$\mathbf{T}_c$	the basis of $\mathbb{T}_c$
$\boldsymbol{S}_t^*$	the element of $\mathbb{T}_c$
$\mathbb{W}_c$	the wrench space of constraints
$\mathbf{W}_c$	the basis of $\mathbb{W}_c$
$\boldsymbol{S}_w^*$	the element of $\mathbb{W}_c$
$\mathbb{T}$	the entire twist space in three-dimensional Euclidean space
$\mathbf{T}$	the basis of $\mathbb{T}$
$\$_t$	the element of $\mathbb{T}$
$\mathbb{W}$	the entire wrench space in three-dimensional Euclidean space
$\mathbf{W}$	the basis of $\mathbb{W}$
$\$_w$	the element of $\mathbb{W}$
$\boldsymbol{S}_{t,i}$	the unit twist associated with ith spring
$\boldsymbol{S}_{w,i}$	the unit wrench associated with ith spring
$\boldsymbol{S}_{t,i}^*$	the unit twist associated with ith constraint
$\boldsymbol{S}_{w,i}^*$	the unit wrench associated with ith constraint
CS(#)	the column space of matrix #
Null(#)	the null space of matrix #
δf_i	the intensity of $\boldsymbol{S}_{w,i}$ $(i = 1,\ 2,\ \cdots j)$
δf_k^*	the intensity of $\boldsymbol{S}_{w,k}^*$ $(k = 1,\ 2,\ \cdots 6-j)$
$\delta\theta_i$	the intensity of $\boldsymbol{S}_{t,i}$ $(i = 1,\ 2,\ \cdots j)$
$\delta\theta_k^*$	the intensity of $\boldsymbol{S}_{t,k}^*$ $(k = 1,\ 2,\ \cdots 6-j)$
$\mathbf{K}$	stiffness matrix
$\mathbf{C}$	compliance matrix
$\mathbf{K}_\theta$	joint stiffness matrix of compliant mechanism
$\mathbf{K}_{\theta,s}$	joint stiffness matrix of compliant mechanism (except constraints)
$\mathbf{C}_\theta$	joint compliance matrix of the compliant mechanism
$\mathbf{C}_{\theta,s}$	joint compliance matrix of compliant mechanism (except constraints)
k_i	the stiffness of ith joint with spring
c_i	the compliance of ith joint with spring
k_i^*	the stiffness of ith constraint
c_i^*	the compliance of ith virtual joint associated with ith constraint
$\boldsymbol{n}_{t,i}$	the ith basis vector of Null($\mathbf{T}_s^{\mathrm{T}}$)
$\boldsymbol{n}_{w,i}$	the ith basis vector of Null($\mathbf{W}_s^{\mathrm{T}}$)
r	length
L	characteristic length
λ	the mean margin of the stiffness errors

stiffness with simple and screw springs. In their recent work [18–20], the geometric construction-based realizations of elastic behaviors with parallel and serial mechanisms were both addressed. With the synthesis procedures presented in [18], the spatial elastic behaviors can be realized by selecting each elastic component in a parallel or serial mechanism based on the geometry of a restricted

space of allowable candidates, and the results show that there are infinite number of solutions that realize a specified elastic behavior. This approach paves the way for realizing a desired elastic behavior by changing the joint stiffnesses and mechanism configuration. Nevertheless, in their work, the rank deficient compliances and constraints were not thoroughly elaborated. Hong and Choi [21] proposed a recursive synthesis method for the realization of a stiffness matrix by connecting the same number of linear and torsional springs in parallel as its rank. Based on the principal axes decomposition, Chen et al. [22] presented an alternative synthesis algorithm for the realization of any symmetric spatial stiffness with two sets of orthogonal springs, namely torsional and screw springs, respectively connected in parallel. Dong et al. [23] proposed an approach for the generalized quality evaluation of grasp stability via contact stiffness. The techniques of stiffness/compliance analysis have been applied to the design and synthesis of robot manipulators by many researchers [24–26]. Note that, all these works provide a solid theoretical foundation for the geometrical interpretation of stiffness/compliance matrix, while the constraints were rarely considered. However, most compliant mechanisms were designed to possess limited degrees of freedom, not full mobility [27,28].

An important task in the initial conceptual design of compliant mechanisms is to identify a suitable arrangement of flexures and actuators for the desired mobility. In other words, the relationships between actuation and constraint spaces, and the stiffness/compliance matrix need to be established so as to determine the desired configuration and actuation scheme. To solve this problem, a variety of constraint-based approaches have been developed for the design of compliant parallel mechanisms [29–32]. Based on screw theory, Hopkins and Culpepper [31–33] proposed a freedom and constraint topology (FACT) approach, which provides an intuitive visualization of the freedom and constraint spaces without mathematical calculation. Yu et al. [34] further presented a modified FACT method by mapping from a geometric concept to physical entities and by combining with other methods, including equivalent compliance mapping, geometric building block, classification and numeration, etc. This method was taken into the practice for flexure modules [35] and flexure systems [34], respectively. Su et al. [36,37] systematically studied the internal relationship between the constraint-based design approach and screw theory, and showed its application to the synthesis and analysis of flexure systems. Furthermore, the concept of line screws with zero pitches was proposed, and used in the synthesis of flexures [38,39]. A symbolic formulation for analytical compliance analysis and synthesis of general flexure mechanisms, including serial chains, parallel chains, or hybrid structures, is presented in [40]. To determinate the layout of actuators, Hopkins and Culpepper [41] proposed a quantitative and graphical design tools that can minimize parasitic errors in parallel flexure systems. Yu et al. [42] pointed out that the constraint wrenches are always linearly independent of actuation forces. Nevertheless, little work has been devoted to the geometrical interpretation of the symmetry properties, especially dualities, of the compliant systems with constraints.

The duality principle exists widely in engineering science [43]. Allowing the engineer, or the designer to transform from one system to a dual system, it can be utilized to simplify the modeling process and discover new designs. As for mechanisms, duality is closely related to the deep symmetry [44] of their structures. Waldron and Hunt [44] first interpreted the duality between kinematics and statics of both serial and parallel manipulators using the virtual work principle. The duality in redundant serial and parallel robots was studied in [45,46]. For planar robots, Duffy [47] conducted an in-depth study of the first-order instantaneous kinematics and statics. Davidson and Hunt [48] further investigated the relations between kinematically equivalent serial and parallel robots. Graphical techniques were also adopted to reveal the dualities of both planar and spatial mechanisms [49,50]. The dual properties between twist and wrench spaces were utilized to construct the generalized Jacobian matrix for lower mobility parallel manipulators [51]. In terms of elastic characteristics, the duality of the eigenscrew decomposition of stiffness/compliance matrix between two equivalent parallel and serial mechanisms was presented in [52]. Ohwovoriole and Roth [53] defined the repelling screw system accompanying the reciprocal screw system to solve the contact problem. In a recent work, Qiu et al. [54] adopted the reciprocal screws in the forward force analysis of Origami mechanisms, which is more or less the same as the statics of parallel mechanisms. A further observation indicates the repelling-screw-based approach provides a geometrical interpretation of mechanical dualities [55]. Therefore, a study of the underlying relationships between repelling screws and the mechanical dualities is needed for understanding comprehensively the geometrical symmetry of compliant mechanisms that correspond to a wider range of mechanism configurations, with either full or limited mobility.

The focus of this work is the correlation between basic concepts underlying the kinematics, statics, motion/constraint and stiffness/compliance of compliant mechanisms, as well as between parallel and serial configurations. Our interest is to provide the reader with a deeper understanding on the dualities of flexible systems in the framework of screw theory. To achieve these goals, the underlying relations among the twist/wrench subspaces of both motion and constraint spaces are analysed and identified. A special case, in which the twist/wrench subspaces of springs are orthogonal to that of constraints, are analysed and further used to adjust the constraint space of compliant parallel mechanisms. Utilizing linear algebra, a method for the construction of the repelling screw system is proposed, upon which the dualities between the kinematics and statics of both parallel and serial compliant mechanisms are revisited and extended. With consideration of constraints, a novel approach for the transformation between parallel and serial compliant mechanisms, along with two methods to adjust the target configuration, are proposed. Examples are presented to demonstrate the application of the proposed approach. Finally, the simulation is carried out to validate the proposed approach, as well as the repelling-screw based interpretation of the dualities of compliant mechanisms.

The rest of this paper is organized as follows. Section 2 briefly introduces the basic concepts of screw, screw operations and repelling screw. The construction of the cofactor matrix of the repelling screw system are presented in Section 3. In Section 4, the twist/wrench spaces, and their subspaces for the general compliant mechanisms are defined, and the dualities between the kinematics and statics of compliant mechanisms with constraints for both serial and parallel configurations are investigated in detail. A novel approach for the configuration transformation between serial and parallel compliant mechanisms along with three typical examples are presented in Section 5. In Section 6, the proposed approach, as well as the duality analysis, are validated by simulation models. The conclusions of this work are presented in Section 7.

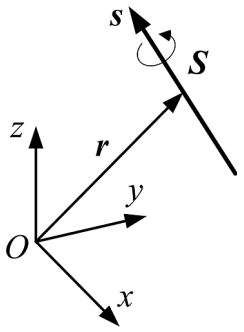

Fig. 1. The direction and position vector of a screw.

2. Screw, interchange operation, and repelling screws

2.1. An introduction to a screw

A screw is a geometrical entity that can be described as a line vector with a pitch that is a scalar coefficient of the second part of the line vector [12,56]. A screw can be represented in the form of a six-dimensional vector with the following definition as

$$\boldsymbol{S} = \begin{bmatrix} \boldsymbol{s} \\ \boldsymbol{s}_0 \end{bmatrix} = \begin{bmatrix} \boldsymbol{s} \\ r \times \boldsymbol{s} + h\boldsymbol{s} \end{bmatrix} \tag{1}$$

where a screw vector (denoted as $\boldsymbol{S}$) consists of an axis vector (denoted as $\boldsymbol{s}$) in a spatial space and a moment vector (denoted as $\boldsymbol{s}_0$) that is the sum of $\boldsymbol{r} \times \boldsymbol{s}$ and $h\boldsymbol{s}$. In three-dimensional Euclidean space, both $\boldsymbol{s}$ and $\boldsymbol{s}_0$ are 3×1 vectors, thus $\boldsymbol{S}$ is a 6×1 vector. $\boldsymbol{r}$ denotes the distance vector between O and an axis vector $\boldsymbol{s}$. h is the screw pitch that is the ratio between the linear and angular speed along an axis. In other words, h is the pitch of $\boldsymbol{s}$ which represents the ratio of the magnitude of $h\boldsymbol{s}$ with respect to that of $\boldsymbol{s}$. A geometrical interpretation of a screw is shown in Fig. 1. It is furthermore possible to see that $\boldsymbol{s} \times (\boldsymbol{r} \times \boldsymbol{s}) = \boldsymbol{r} \parallel \boldsymbol{s} \parallel$, and therefore, $\boldsymbol{r}$ is provided as

$$\boldsymbol{r} = \frac{\boldsymbol{s} \times \boldsymbol{s}_0}{\parallel \boldsymbol{s} \parallel^2} \tag{2}$$

Similarly, by taking the scalar product of $\boldsymbol{s}$ with $\boldsymbol{s}_0$ we obtain

$$\boldsymbol{s}^{\mathrm{T}}\boldsymbol{s}_0 = \boldsymbol{s}^{\mathrm{T}}(\boldsymbol{r} \times \boldsymbol{s} + h\boldsymbol{s}) = \boldsymbol{s}^{\mathrm{T}}(\boldsymbol{r} \times \boldsymbol{s}) + h\boldsymbol{s}^{\mathrm{T}}\boldsymbol{s} \tag{3}$$

As the first term $\boldsymbol{s}^{\mathrm{T}}(\boldsymbol{r} \times \boldsymbol{s})$ on the right side is zero, based on the property of the mixed product, we have

$$h = \frac{\boldsymbol{s}^{\mathrm{T}}\boldsymbol{s}_0}{\parallel \boldsymbol{s} \parallel^2} \tag{4}$$

Support for the axis vector that $\boldsymbol{s} = 0$, the screw is defined to have an infinite pitch, which has the form

$$\boldsymbol{S} = \begin{bmatrix} \boldsymbol{0} \\ h\boldsymbol{s} \end{bmatrix} \tag{5}$$

where the dual part $h\boldsymbol{s}$ represents the axis vector.

2.2. Screw interchange operation

The general screw definition given in Eq. (1) is actually described using the Plücker ray coordinate frame [57]. It will be shown this form of a screw is mostly used to represent a wrench in mechanism analysis later. There also exists another form of a screw that exchanges the first and second part of the screw in Eq. (1). This new form of a screw is said to be represented in a Plücker axis coordinate frame, which can be written as

$$\boldsymbol{S}_{axis} = \begin{bmatrix} \boldsymbol{s}_0 \\ \boldsymbol{s} \end{bmatrix} \tag{6}$$

In contrast to the Plücker ray coordinated screw, mostly $\boldsymbol{S}_{axis}$ is used for representing a twist in mechanism analysis. The relationship between $\boldsymbol{S}_{axis}$ and $\boldsymbol{S}$ can be written as

$$\boldsymbol{S}_{axis} = \boldsymbol{\Delta}\boldsymbol{S} \tag{7}$$

where $\boldsymbol{\Delta}$ is the elliptical polar operator [58], which has the form

$$\boldsymbol{\Delta} = \begin{bmatrix} \mathbf{0} & \mathbf{I}_3 \\ \mathbf{I}_3 & \mathbf{0} \end{bmatrix} \tag{8}$$

where $\mathbf{0}$ is a 3×3 zero matrix, and $\mathbf{I}_3$ is a 3×3 identity matrix. $\boldsymbol{\Delta}$ has some properties as the following

$$\boldsymbol{\Delta} = \boldsymbol{\Delta}^{-1} \tag{9a}$$

$$\boldsymbol{\Delta} = \boldsymbol{\Delta}^{\mathrm{T}} \tag{9b}$$

$$\boldsymbol{\Delta}\boldsymbol{\Delta} = \mathbf{I}_3 \tag{9c}$$

2.3. An introduction to repelling screws

Similar to the reciprocal screw system, a new type of screw system can be established according to the concept of repelling screws [53]. For a given screw system $\mathbb{S}$, its repelling screw system is symbolized as $\mathbb{S}_r$. Any repelling screw $\boldsymbol{S}_{r,j}$ that belongs to $\mathbb{S}_r$ is defined to have a positive reciprocal product with $\boldsymbol{S}_i$ ($\boldsymbol{S}_i \in \mathbb{S}$) when $j = i$, and its reciprocal product with other screws are zero [54]. This can be described as

$$\boldsymbol{S}_{r,j} = \begin{cases} \left(\boldsymbol{S}_{r,j}\right)^{\mathrm{T}} \boldsymbol{S}_i > 0, & i = j \\ \left(\boldsymbol{S}_{r,j}\right)^{T} \boldsymbol{S}_i = 0, & i \neq j \end{cases} \tag{10}$$

As a result, we can always find n repelling screws for a given screw system to establish the repelling screw system

$$\mathbb{S}_r = \left\{\boldsymbol{S}_{r,1},\ \boldsymbol{S}_{r,2},\ \ldots,\ \boldsymbol{S}_{r,n}\right\} \tag{11}$$

Also, the dimension of repelling screw system is equal to that of the given screw system

$$\dim(\mathbb{S}_r) = \dim(\mathbb{S}) = n \tag{12}$$

Further it will be shown that repelling screws are particularly useful in the duality analysis of compliant mechanisms.

3. Constructions of the cofactor matrices of screw system and its repelling screw system

3.1. Repelling screws of general full-rank space

For an invertible 6×6 matrix $\mathbf{J}$, it can be written as

$$\mathbf{J} = [\boldsymbol{S}_1\ \boldsymbol{S}_2\ \cdots\ \boldsymbol{S}_6] \tag{13}$$

with $\boldsymbol{S}_j = [l_j\ m_j\ n_j\ P_j\ Q_j\ R_j\ ]^{\mathrm{T}}$.

According to the **Cramer's rule**, the inverse of $\mathbf{J}$ can be calculated analytically using the determinant and matrix of cofactors of $\mathbf{J}$, which has the form as

$$\mathbf{J}^{-1} = \frac{1}{|\mathbf{J}|}\mathbf{R}^{\mathrm{T}} = \frac{1}{|\mathbf{J}|}\begin{bmatrix} r_{11} & r_{12} & \cdots & r_{16} \\ r_{21} & r_{22} & \cdots & r_{26} \\ \vdots & \vdots & \ddots & \vdots \\ r_{61} & r_{62} & \cdots & r_{66} \end{bmatrix}^{\mathrm{T}} \tag{14}$$

where r_{ij} is the cofactor of the $(i.j) - th$ element of $\mathbf{J}$. For example, we have

$$r_{11} = (-1)^{1+1}\begin{vmatrix} m_2 & m_3 & m_4 & m_5 & m_6 \\ n_2 & n_3 & n_4 & n_5 & n_6 \\ P_2 & P_3 & P_4 & P_5 & P_6 \\ Q_2 & Q_3 & Q_4 & Q_5 & Q_6 \\ R_2 & R_3 & R_4 & R_5 & R_6 \end{vmatrix} \tag{15}$$

and the rest elements are the same as this. Thus, the inverse of $\mathbf{J}^T$ has the form as

$$\left(\mathbf{J}^{\mathrm{T}}\right)^{-1} = \frac{1}{|\mathbf{J}|}\mathbf{R} = \frac{1}{|\mathbf{J}|}\begin{bmatrix} r_{11} & r_{12} & \cdots & r_{16} \\ r_{21} & r_{22} & \cdots & r_{26} \\ \vdots & \vdots & \ddots & \vdots \\ r_{61} & r_{62} & \cdots & r_{66} \end{bmatrix} \tag{16}$$

If we further write $\mathbf{R}$ in the following form

$$\mathbf{R} = \begin{bmatrix} \boldsymbol{S}_{r,1} & \boldsymbol{S}_{r,2} & \cdots & \boldsymbol{S}_{r,6} \end{bmatrix} \tag{17}$$

According to the **Laplace's formula of cofactor expansion of the determinant**, the cofactor expansion along the $j-th$ column of $\mathbf{J}$ can be written as

$$\left(\boldsymbol{S}_{r,j}\right)^{\mathrm{T}}\boldsymbol{S}_j = r_{1j}l_j + r_{2j}m_j + r_{3j}n_j + r_{4j}P_j + r_{5j}Q_j + r_{6j}R_j = |\mathbf{J}| \tag{18}$$

Then for the rest of screws $\boldsymbol{S}_k (k \neq j)$, we have

$$\left(\boldsymbol{S}_{r,j}\right)^{\mathrm{T}}\boldsymbol{S}_k = r_{1j}l_k + r_{2j}m_k + r_{3j}n_k + r_{4j}P_k + r_{5j}Q_k + r_{6j}R_k = \left|\boldsymbol{S}_1 \ \cdots \ \boldsymbol{S}_{j-1}\boldsymbol{S}_k\boldsymbol{S}_{j+1} \ \cdots \ \boldsymbol{S}_6\right| = 0 \tag{19}$$

Thus, we prove $\boldsymbol{S}_{r,j}$ is the repelling screw of screw $\boldsymbol{S}_j (j = 1, \ \cdots, \ 6)$ according to the definition of repelling screw. Note that, $\boldsymbol{S}_{r,i}$ is not a unit screw in this section. Further Eq. (18) makes it possible to write Eq. (16) in another form as

$$\left(\mathbf{J}^{\mathrm{T}}\right)^{-1} = \left[\frac{\boldsymbol{S}_{r,1}}{\left(\boldsymbol{S}_{r,1}\right)^{\mathrm{T}}\boldsymbol{S}_1} \ \frac{\boldsymbol{S}_{r,2}}{\left(\boldsymbol{S}_{r,2}\right)^{\mathrm{T}}\boldsymbol{S}_2} \ \cdots \ \frac{\boldsymbol{S}_{r,6}}{\left(\boldsymbol{S}_{r,6}\right)^{\mathrm{T}}\boldsymbol{S}_6}\right] \tag{20}$$

Eq. (20) gives us the geometrical interpretation of the inverse of $\mathbf{J}^{\mathrm{T}}$. In Eq. (20), $\left(\boldsymbol{S}_{r,i}\right)^{\mathrm{T}}\boldsymbol{S}_i \neq 0$. Note that, as $\boldsymbol{S}_{r,i}$ exists in both the numerator and denominator of the item $\frac{\boldsymbol{S}_{r,i}}{\left(\boldsymbol{S}_{r,i}\right)^{\mathrm{T}}\boldsymbol{S}_i}$ in matrix $\left(\mathbf{J}^{\mathrm{T}}\right)^{-1}$. The different signs of the product $\left(\boldsymbol{S}_{r,i}\right)^{\mathrm{T}}\boldsymbol{S}_i$ indicate different directions of $\boldsymbol{S}_{r,i}$. In this paper, without loss of generality, we assume that $\left(\boldsymbol{S}_{r,i}\right)^{\mathrm{T}}\boldsymbol{S}_i > 0$, which implies that the unit motion (force) corresponding to the twist (wrench) $\boldsymbol{S}_i$ always does positive work through the wrench (twist) $\boldsymbol{S}_{r,i}$.

3.2. Repelling screws of the matrix with rank less than 6

For a matrix with a rank less than six, it has

$$\mathbf{J} = \begin{bmatrix} \boldsymbol{S}_1 & \boldsymbol{S}_2 & \cdots & \boldsymbol{S}_j \end{bmatrix} \tag{21}$$

where j is the number of independent screws and $j < 6$. As a result, it can always find $(6-j)$ screws that span the null space of $\mathbf{J}^{\mathrm{T}}$. According to linear algebra [59], the column space of $\mathbf{J}$ is defined as

$$\mathrm{CS}(\mathbf{J}) = \mathrm{Span}\left(\boldsymbol{S}_1, \ \boldsymbol{S}_2, \ \cdots \ \boldsymbol{S}_j\right) \tag{22}$$

The null space of $\mathbf{J}^{\mathrm{T}}$ can be expressed as

$$\mathrm{Null}\left(\mathbf{J}^{\mathrm{T}}\right) = \ \mathrm{Span}\left(\boldsymbol{S}_1^*, \ \boldsymbol{S}_2^*, \ \cdots \ \boldsymbol{S}_{6-j}^*\right) \tag{23}$$

As $\mathrm{CS}(\mathbf{J})$ is orthogonal to $\mathrm{Null}(\mathbf{J}^{\mathrm{T}})$, namely $\mathrm{CS}(\mathbf{J}) = \mathrm{Null}\left(\mathbf{J}^{\mathrm{T}}\right)^{\perp}$, and $\dim(\mathrm{CS}(\mathbf{J}))+\dim(\mathrm{Null}(\mathbf{J}^{\mathrm{T}})) = 6$. Thus, the following relationship holds

$$\mathbf{J}^{\mathrm{T}}\boldsymbol{S}_k^* = 0, \ k = 1, \ 2, \ \cdots 6-j \tag{24}$$

The null space of matrix $\mathbf{J}^{\mathrm{T}}$ can be obtained by several available approaches, such as Gram Schmidt orthogonalization [60,61], augmentation matrix approach [62,63], and the observation method [64] for mechanisms. We can construct an augmented matrix $\mathbf{J}^*$, which consists of 6-j linearly independent screws in $\mathrm{Null}(\mathbf{J}^{\mathrm{T}})$ and has the form as

$$\mathbf{J}^* = \begin{bmatrix} \boldsymbol{S}_1^* & \boldsymbol{S}_2^* & \cdots & \boldsymbol{S}_{6-j}^* \end{bmatrix} \tag{25}$$

Then we can obtain a new matrix $\mathbf{G}$ which is 6×6 full rank matrix, and it can be written as

$$\mathbf{G} = [\mathbf{J} \ \mathbf{J}^*] \tag{26}$$

Since $\mathbf{G}$ is full rank, according to the inverse of full rank 6×6 matrix developed in Section 3.1, we can always find the inverse of $\mathbf{G}^{\mathrm{T}}$ using repelling screws, which can be written as

$$\left(\mathbf{G}^{\mathrm{T}}\right)^{-1} = [\mathbf{A}, \ \mathbf{B}] = \left[\frac{\boldsymbol{S}_{r,1}}{\left(\boldsymbol{S}_{r,1}\right)^{T}\boldsymbol{S}_1} \ \cdots \ \frac{\boldsymbol{S}_{r,j}}{\left(\boldsymbol{S}_{r,j}\right)^{T}\boldsymbol{S}_j}, \ \frac{\boldsymbol{S}_{r,1}^*}{\left(\boldsymbol{S}_{r,1}^*\right)^{T}\boldsymbol{S}_1^*} \ \cdots \ \frac{\boldsymbol{S}_{r,6-j}^*}{\left(\boldsymbol{S}_{r,6-j}^*\right)^{T}\boldsymbol{S}_{6-j}^*}\right] \tag{27}$$

On the other hand, we also have

$$\left(\mathbf{G}^{\mathrm{T}}\right)^{-1} = \mathbf{G}\left(\mathbf{G}^{\mathrm{T}}\mathbf{G}\right)^{-1} = [\mathbf{J} \ \mathbf{J}^*]\left(\begin{bmatrix} \mathbf{J}^{\mathrm{T}} \\ \left(\mathbf{J}^*\right)^{\mathrm{T}} \end{bmatrix}[\mathbf{J} \ \ \mathbf{J}^*]\right)^{-1} = [\mathbf{J} \ \mathbf{J}^*]\begin{bmatrix} \mathbf{J}^{\mathrm{T}}\mathbf{J} & \mathbf{J}^{\mathrm{T}}\mathbf{J}^* \\ \left(\mathbf{J}^*\right)^{\mathrm{T}}\mathbf{J} & \left(\mathbf{J}^*\right)^{\mathrm{T}}\mathbf{J}^* \end{bmatrix}^{-1} \tag{28}$$

According to Eq. (24), Eq. (28) can be further simplified as

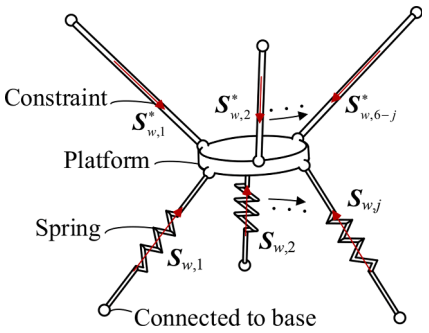

Fig. 2. Schematic diagram of general compliant parallel mechanism with constraints.

$$\left(\mathbf{G}^{\mathrm{T}}\right)^{-1}=[\mathbf{J}\ \mathbf{J}^{*}]\begin{bmatrix}\mathbf{J}^{\mathrm{T}}\mathbf{J} & \mathbf{0}\\ \mathbf{0} & (\mathbf{J}^{*})^{\mathrm{T}}\mathbf{J}^{*}\end{bmatrix}^{-1}=\left[\mathbf{J}\left(\mathbf{J}^{\mathrm{T}}\mathbf{J}\right)^{-1}\ \mathbf{J}^{*}\left((\mathbf{J}^{*})^{\mathrm{T}}\mathbf{J}^{*}\right)^{-1}\right] \tag{29}$$

Both Eqs. (27) and (29) give us the formulation of the inverse of $\mathbf{G}^{\mathrm{T}}$. Due to its uniqueness, we can further conclude that

$$\mathbf{A}=\ \mathbf{J}\left(\mathbf{J}^{\mathrm{T}}\mathbf{J}\right)^{-1} \tag{30a}$$

$$\mathbf{B}=\mathbf{J}^{*}\left((\mathbf{J}^{*})^{\mathrm{T}}\mathbf{J}^{*}\right)^{-1} \tag{30b}$$

Eq. (30) tells us **A** is determined by **J** if Eq. (24) satisfies, which means the pseudo inverse of matrix **J** represented by corresponding repelling screws are uniquely determined no matter how augmented matrix $\mathbf{J}^{*}$ is selected. Also, the geometrical meaning of pseudo inverse of **J** can be interpreted using the repelling screw-based matrix **A** according to Eq. (27).

4. Kinematics and statics of compliant mechanisms with constraints

In this section, the twist/wrench spaces and their subspaces that correspond to both spring displacements and constraints are defined for compliant mechanisms. Subsequently, the duality between the kinematics and statics of compliant mechanism with constraints is investigated. The relationships among the twist and wrench spaces of compliant mechanisms for both serial and parallel configurations are revisited and extended.

4.1. Twist/Wrench spaces, and their subspaces of the compliant mechanism with constraints

Referring to Refs. [51,65,66], the set of permitted motions (or twists) spans a j dimensional vector space $\mathbb{T}_s$, known as the twist space of springs, the basis of which can be denoted by the matrix $\mathbf{T}_s=[\boldsymbol{S}_{t,1},\boldsymbol{S}_{t,2},\cdots,\boldsymbol{S}_{t,j}]$. The element of $\mathbb{T}_s$ is denoted by $\boldsymbol{S}_t$, and $\boldsymbol{S}_t=\mathrm{Span}(\boldsymbol{S}_{t,1},\ \boldsymbol{S}_{t,2},\ \cdots\ \boldsymbol{S}_{t,j})$. Similarly, the set of restricted motions spans a $6-j$ dimensional vector space $\mathbb{T}_c$, known as the twist space of constraints, the basis of which can be denoted by the matrix $\mathbf{T}_c=[\boldsymbol{S}^{*}_{t,1},\boldsymbol{S}^{*}_{t,2},\cdots,\boldsymbol{S}^{*}_{t,6-j}]$. The element of $\mathbb{T}_c$ is denoted by $\boldsymbol{S}^{*}_t$, and $\boldsymbol{S}^{*}_t=\mathrm{Span}(\boldsymbol{S}^{*}_{t,1},\ \boldsymbol{S}^{*}_{t,2},\cdots,\boldsymbol{S}^{*}_{t,6-j})$. For compliant mechanisms, the twists of constraints lead to the errors caused by component compliances. The entire set of twists in three-dimensional Euclidean space spans a 6 dimensional vector space $\mathbb{T}$, and its basis $\mathbf{T}=[\mathbf{T}_s\ \mathbf{T}_c]$. The element of $\mathbb{T}$ is denoted by $\$_t$, and $\$_t=\mathrm{Span}(\boldsymbol{S}_{t,1},\ \cdots,\boldsymbol{S}_{t,j},\ \boldsymbol{S}^{*}_{t,1},\ \cdots,\ \boldsymbol{S}^{*}_{t,6-j})$.

In analogy to the subspaces of twists, the set of the wrenches generated by springs spans a j dimensional vector space $\mathbb{W}_s$, known as the wrench space of springs, the basis of which can be denoted by the matrix $\mathbf{W}_s=[\boldsymbol{S}_{w,1}\ \boldsymbol{S}_{w,2}\ \cdots\ \boldsymbol{S}_{w,j}]$. The element of $\mathbb{W}_s$ is denoted by $\boldsymbol{S}_w$, and $\boldsymbol{S}_w=\mathrm{Span}(\boldsymbol{S}_{w,1}\ \boldsymbol{S}_{w,2}\ \cdots\ \boldsymbol{S}_{w,j})$. Similarly, the set of the wrenches induced by the twists of constraints spans a $6-j$ dimensional vector space $\mathbb{W}_c$, known as the wrench space of constraints, the basis of which can be denoted by the matrix $\mathbf{W}_c=[\boldsymbol{S}^{*}_{w,1}\ \boldsymbol{S}^{*}_{w,2}\ \cdots\ \boldsymbol{S}^{*}_{w,6-j}]$. The element of $\mathbb{W}_c$ is denoted by $\boldsymbol{S}^{*}_w$, and $\boldsymbol{S}^{*}_w=\mathrm{Span}(\boldsymbol{S}^{*}_{w,1},\ \boldsymbol{S}^{*}_{w,2},\cdots,\boldsymbol{S}^{*}_{w,6-j})$. The entire set of wrenches in 3D space spans a 6 dimensional vector space $\mathbb{W}$, and its basis $\mathbf{W}=[\mathbf{W}_s\ \mathbf{W}_c]$. The element of $\mathbb{W}$ is denoted by $\$_w$, and $\$_w=\mathrm{Span}(\boldsymbol{S}_{w,1},\ \cdots,\boldsymbol{S}_{w,j},\ \boldsymbol{S}^{*}_{w,1},\ \cdots,\ \boldsymbol{S}^{*}_{w,6-j})$.

Note that, in this work, the unit wrench $\boldsymbol{S}_{w,i}$ / $\boldsymbol{S}^{*}_{w,i}$ is described with Plücker ray coordinates, while the unit twist $\boldsymbol{S}_{t,i}$ / $\boldsymbol{S}^{*}_{t,i}$ is described with the Plücker axis coordinates. Thus the reciprocal product between a wrench and a twist is obtained by dot product. As $\mathbb{T}_s\cap\mathbb{T}_c=\varnothing$, the basis vectors in $\mathbf{T}_s$ and $\mathbf{T}_c$ are linearly independent to each other. The same situation exists between the basis vectors in $\mathbf{W}_s$ and $\mathbf{W}_c$.

In the work [51], the following relationships were presented

$$\mathbb{T}_s=\mathbb{W}_c^{\perp};\ \mathbb{T}_c=\mathbb{W}_s^{\perp};\ \mathbb{T}_s=\mathbb{W}_s^{*};\ \mathbb{T}_c=\mathbb{W}_c^{*} \tag{31}$$

where "$\perp$" indicates that the two subspaces are orthogonal to each other, and "$*$" indicates the two subspaces are dual to each other. In fact, the statement that $\mathbb{T}_s=\mathbb{W}_s^{*}$ and $\mathbb{T}_c=\mathbb{W}_c^{*}$ is not rigorous, as $\mathbb{T}_s$ ($\mathbb{T}_c$) is influenced by $\mathbf{W}_c$ ($\mathbf{W}_s$). To be more precise, the relationship between the twist and wrench spaces is given as $\mathbb{T}=\mathbb{W}^{*}$, which holds for general parallel and serial types of mechanisms. It is

noteworthy that this relationship remains invariant with the change of coordinate system.

4.2. Kinematics and statics of parallel compliant mechanisms with constraints

4.2.1. Kinematics and statics of general parallel compliant mechanisms

For parallel compliant mechanisms, as shown in Fig. 2, the wrench space $\mathbf{W}$ of both springs and constraints are readily obtained. The relation between infinitesimal motion and force expressed in duality form is given as [44]

$$\$_w = \mathbf{W}\delta\boldsymbol{f} \tag{32a}$$

$$\$_t = \left(\mathbf{W}^{\mathrm{T}}\right)^{-1}\delta\boldsymbol{\theta} \tag{32b}$$

with

$$\mathbf{W} = [\mathbf{W}_s\ \mathbf{W}_c]$$

$$\delta\boldsymbol{f} = \left[\delta f_1\ \cdots\ \delta f_j\ \delta f_1^*\ \cdots\ \delta f_{6-j}^*\right]^{\mathrm{T}}$$

$$\delta\boldsymbol{\theta} = \left[\delta\theta_1\ \cdots\ \delta\theta_j\ \delta\theta_1^*\ \cdots\ \delta\theta_{6-j}^*\right]^{\mathrm{T}}.$$

where δf_i and δf_k^* denote the intensity of $\boldsymbol{S}_{w,i}$ $(i=1,\ 2,\ \cdots j)$ and $\boldsymbol{S}_{w,k}^*$ $(k=1,\ 2,\ \cdots 6-j)$. $\delta\theta_i$ and $\delta\theta_k^*$ denote the intensity of $\boldsymbol{S}_{t,i}$ $(i=1,\ 2,\ \cdots j)$ and $\boldsymbol{S}_{t,k}^*$ $(k=1,\ 2,\ \cdots 6-j)$, and they can be interpreted as infinitesimal displacement or speed for the analysis of deflection or velocity, respectively. Referring to [67], the inverse of the transpose of $\mathbf{W}$ be represented as

$$\left(\mathbf{W}^{\mathrm{T}}\right)^{-1} = [\mathbf{T}_{\mathrm{A}}\ \mathbf{T}_{\mathrm{B}}] = \mathbf{W}\left(\mathbf{W}^{\mathrm{T}}\mathbf{W}\right)^{-1} = [\mathbf{W}_s\ \mathbf{W}_c]\left(\begin{bmatrix}\mathbf{W}_s^{\mathrm{T}}\\ \mathbf{W}_c^{\mathrm{T}}\end{bmatrix}[\mathbf{W}_s\ \mathbf{W}_c]\right)^{-1} = [\mathbf{W}_s\ \mathbf{W}_c]\begin{bmatrix}\mathbf{W}_s^{\mathrm{T}}\mathbf{W}_s & \mathbf{W}_s^{\mathrm{T}}\mathbf{W}_c\\ \mathbf{W}_c^{\mathrm{T}}\mathbf{W}_s & \mathbf{W}_c^{\mathrm{T}}\mathbf{W}_c\end{bmatrix}^{-1}$$

$$= [\mathbf{W}_s\ \mathbf{W}_c]\begin{bmatrix}\mathbf{C}_1^{-1} & -\left(\mathbf{W}_s^{\mathrm{T}}\mathbf{W}_s\right)^{-1}\mathbf{W}_s^{\mathrm{T}}\mathbf{W}_c\mathbf{C}_2^{-1}\\ -\mathbf{C}_2^{-1}\mathbf{W}_c^{\mathrm{T}}\mathbf{W}_s\left(\mathbf{W}_s^{\mathrm{T}}\mathbf{W}_s\right)^{-1} & \mathbf{C}_2^{-1}\end{bmatrix}$$

$$= \begin{bmatrix}\mathbf{W}_s\mathbf{C}_1^{-1} - \mathbf{W}_c\mathbf{C}_2^{-1}\mathbf{W}_c^{\mathrm{T}}\mathbf{W}_s\left(\mathbf{W}_s^{\mathrm{T}}\mathbf{W}_s\right)^{-1} & \mathbf{W}_c\mathbf{C}_2^{-1} - \mathbf{W}_s\left(\mathbf{W}_s^{\mathrm{T}}\mathbf{W}_s\right)^{-1}\mathbf{W}_s^{\mathrm{T}}\mathbf{W}_c\mathbf{C}_2^{-1}\end{bmatrix} \tag{33}$$

Thus

$$\mathbf{T}_{\mathrm{A}} = \mathbf{W}_s\mathbf{C}_1^{-1} - \mathbf{W}_c\mathbf{C}_2^{-1}\mathbf{W}_c^{\mathrm{T}}\mathbf{W}_s\left(\mathbf{W}_s^{\mathrm{T}}\mathbf{W}_s\right)^{-1} \tag{34a}$$

$$\mathbf{T}_{\mathrm{B}} = \mathbf{W}_c\mathbf{C}_2^{-1} - \mathbf{W}_s\left(\mathbf{W}_s^{\mathrm{T}}\mathbf{W}_s\right)^{-1}\mathbf{W}_s^{\mathrm{T}}\mathbf{W}_c\mathbf{C}_2^{-1} \tag{34b}$$

where

$$\mathbf{C}_1 = \left(\mathbf{W}_s^{\mathrm{T}}\mathbf{W}_s - \mathbf{W}_s^{\mathrm{T}}\mathbf{W}_c\left(\mathbf{W}_c^{\mathrm{T}}\mathbf{W}_c\right)^{-1}\mathbf{W}_c^{\mathrm{T}}\mathbf{W}_s\right)$$

$$\mathbf{C}_2 = \left(\mathbf{W}_c^{\mathrm{T}}\mathbf{W}_c - \mathbf{W}_c^{\mathrm{T}}\mathbf{W}_s\left(\mathbf{W}_s^{\mathrm{T}}\mathbf{W}_s\right)^{-1}\mathbf{W}_s^{\mathrm{T}}\mathbf{W}_c\right).$$

Subsequently, we proceed to the calculation of the repelling screws $\boldsymbol{S}_{t,i}$ $(i=1,\ 2,\ \cdots j)$ and $\boldsymbol{S}_{t,k}^*$ $(k=1,\ 2,\ \cdots 6-j)$ for $\boldsymbol{S}_{w,i}$ $(i=1,\ 2,\ \cdots j)$ and $\boldsymbol{S}_{w,k}^*$ $(k=1,\ 2,\ \cdots 6-j)$. According to Eq. (20), we have

$$\mathbf{T}_{\mathrm{A}} = \left[\frac{\boldsymbol{S}_{t,1}}{\left(\boldsymbol{S}_{t,1}\right)^{\mathrm{T}}\boldsymbol{S}_{w,1}}\ \cdots\ \frac{\boldsymbol{S}_{t,j}}{\left(\boldsymbol{S}_{t,j}\right)^{\mathrm{T}}\boldsymbol{S}_{w,j}}\right] \tag{35a}$$

$$\mathbf{T}_{\mathrm{B}} = \left[\frac{\boldsymbol{S}_{t,1}^*}{\left(\boldsymbol{S}_{t,1}^*\right)^{\mathrm{T}}\boldsymbol{S}_{w,1}^*}\ \cdots\ \frac{\boldsymbol{S}_{t,6-j}^*}{\left(\boldsymbol{S}_{t,6-j}^*\right)^{\mathrm{T}}\boldsymbol{S}_{w,6-j}^*}\right] \tag{35b}$$

Thus, the repelling screw system, namely the twist space of springs and constraints can be written as

$$\mathbf{T} = [\mathbf{T}_s\quad \mathbf{T}_c] = \left(\mathbf{W}^{\mathrm{T}}\right)^{-1}\boldsymbol{\Lambda}_t \tag{36a}$$

$$\mathbf{T}_s = \mathbf{T}_{\mathrm{A}}\boldsymbol{\Lambda}_{t,s} \tag{36b}$$

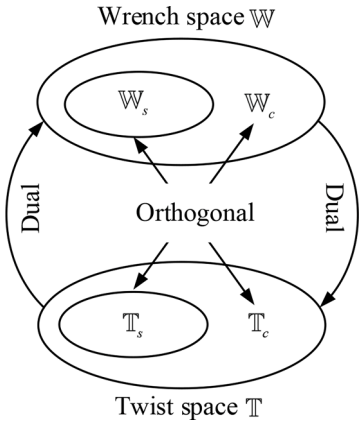

Fig. 3. Relations among twist/wrench spaces, and their subspaces of the general parallel compliant mechanism with constraint [51,65,66].

$$\mathbf{T}_c = \mathbf{T}_{\mathrm{B}}\boldsymbol{\Lambda}_{t,c} \tag{36c}$$

where

$$\boldsymbol{\Lambda}_t = \mathrm{diag}\left[\left(\boldsymbol{S}_{t,1}\right)^{\mathrm{T}}\boldsymbol{S}_{w,1} \ \cdots \ \left(\boldsymbol{S}_{t,j}\right)^{\mathrm{T}}\boldsymbol{S}_{w,j} \ \left(\boldsymbol{S}^*_{t,1}\right)^{\mathrm{T}}\boldsymbol{S}^*_{w,1} \ \cdots \ \left(\boldsymbol{S}^*_{t,6-j}\right)^{\mathrm{T}}\boldsymbol{S}^*_{w,6-j}\right]$$

$$\boldsymbol{\Lambda}_{t,s} = \mathrm{diag}\left[\left(\boldsymbol{S}_{t,1}\right)^{\mathrm{T}}\boldsymbol{S}_{w,1} \ \cdots \ \left(\boldsymbol{S}_{t,j}\right)^{\mathrm{T}}\boldsymbol{S}_{w,j}\right]$$

$$\boldsymbol{\Lambda}_{t,c} = \mathrm{diag}\left[\left(\boldsymbol{S}^*_{t,1}\right)^{\mathrm{T}}\boldsymbol{S}^*_{w,1} \ \cdots \ \left(\boldsymbol{S}^*_{t,6-j}\right)^{\mathrm{T}}\boldsymbol{S}^*_{w,6-j}\right].$$

The physical meaning behind the repelling screws can be interpreted as that the displacement (deformation) associated with the spring (constraint) of ith limb leads to the motion related to the twist $\boldsymbol{S}_{t,i}$ ($\boldsymbol{S}^*_{t,i}$). Note that, if the errors caused by the constraint compliance are not considered, there does not exist displacement along the constraint link, the value of $\delta\theta^*_k$ is always equal to zero. Accordingly, Eq. (32b) can be written as

$$\$_t = \mathbf{T}_s\left(\boldsymbol{\Lambda}_{t,s}\right)^{-1}\delta\boldsymbol{\theta}_s \tag{37}$$

with $\delta\boldsymbol{\theta}_s = [\delta\theta_1 \ \cdots \ \delta\theta_j]^T$.

According to Eqs. (35) and (36), $\mathbf{T}_s$ and $\mathbf{T}_c$ can be interpreted as the normalized form of $\mathbf{T}_{\mathrm{A}}$ and $\mathbf{T}_{\mathrm{B}}$, respectively. From Eq. (34), we can conclude that $\mathbf{W}_c$ has effect on $\mathbf{T}_s$, and $\mathbf{T}_c$ is influenced by $\mathbf{W}_s$. The arrangement of constraints affects the twist space of springs, thus the conclusion that $\mathbb{T}_s$ ($\mathbb{T}_c$) and $\mathbb{W}_s$ ($\mathbb{W}_c$) are dual to each other is weakling. The relationships among the twist/wrench subspaces of the general compliant parallel mechanism are depicted in Fig. 3.

4.2.2. Orthogonal twist/wrench subspaces of constraints and springs-a special case for parallel configuration

In the preceding section, the general case of dualities between the kinematics and statics of general compliant parallel mechanisms are analysed and illustrated. For parallel compliant mechanisms, the twists in the operation space vary with respect to the changes of the constraint mode. Some constraint modes may lead to bad performances, such as small workspace, large errors, and internal forces. Moreover, compliant mechanisms are mostly designed to translate along selected directions and rotate about specified axes [68–73]. In most designs of compliant mechanisms, the twist space of springs is orthogonal to the twist space of constraints, and the same situation exists between the wrench spaces of both springs and constraints, which indicates $\boldsymbol{S}_t^{\mathrm{T}}\boldsymbol{S}^*_t = 0$ and $\boldsymbol{S}_w^{\mathrm{T}}\boldsymbol{S}^*_w = 0$. Therefore, it is of significance to investigate the special case that the twist subspace of constraints $\mathbb{T}_c$ is the orthogonal complement of the twist subspace of springs $\mathbb{T}_s$, and the wrench subspace of constraints $\mathbb{W}_c$ is the orthogonal complement of the wrench subspace of springs $\mathbb{W}_s$. For this special case, the relationships among the twist/wrench subspaces of constraints and springs are given as

$$\mathbf{T}_s^{\mathrm{T}}\mathbf{T}_c = 0 \tag{38a}$$

$$\mathbf{W}_s^{\mathrm{T}}\mathbf{W}_c = 0 \tag{38b}$$

According to Eqs. (22)–(24), $\boldsymbol{S}^*_w$, namely the element of $\mathbb{W}_c$, belongs to the null space of $\mathbf{W}_s^{\mathrm{T}}$. Similar to Eq. (29), the inverse of the transpose of $\mathbf{W}$ be represented as

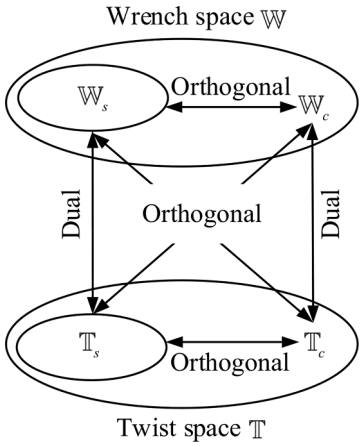

Fig. 4. Relations among twist and wrench subspaces of the parallel compliant mechanism when the twist/wrench subspaces of springs are orthogonal to that of constraints.

$$\left(\mathbf{W}^{\mathrm{T}}\right)^{-1} = [\mathbf{T}_{\mathrm{A}}\ \mathbf{T}_{\mathrm{B}}] = [\mathbf{W}_s\ \mathbf{W}_c]\begin{bmatrix}\mathbf{W}_s^{\mathrm{T}}\mathbf{W}_s & \mathbf{0}\\ \mathbf{0} & \mathbf{W}_c^{\mathrm{T}}\mathbf{W}_c\end{bmatrix}^{-1} \tag{39}$$

$$= \left[\mathbf{W}_s\left(\mathbf{W}_s^{\mathrm{T}}\mathbf{W}_s\right)^{-1}\ \mathbf{W}_c\left(\mathbf{W}_c^{\mathrm{T}}\mathbf{W}_c\right)^{-1}\right]$$

Thus

$$\mathbf{T}_{\mathrm{A}} = \mathbf{W}_s\left(\mathbf{W}_s^{\mathrm{T}}\mathbf{W}_s\right)^{-1} \tag{40a}$$

$$\mathbf{T}_{\mathrm{B}} = \mathbf{W}_c\left(\mathbf{W}_c^{\mathrm{T}}\mathbf{W}_c\right)^{-1} \tag{40b}$$

Subsequently, we move to the calculation of the repelling screws $\boldsymbol{S}_{t,i}$ $(i=1,\ 2,\ \cdots j)$ and $\boldsymbol{S}^*_{t,k}$ $(k=1,\ 2,\ \cdots 6-j)$ for $\boldsymbol{S}_{w,i}$ $(i=1,\ 2,\ \cdots j)$ and $\boldsymbol{S}^*_{w,k}$ $(k=1,\ 2,\ \cdots 6-j)$. According to Eq. (27), we have

$$\mathbf{T}_{\mathrm{A}} = \mathbf{W}_s\left(\mathbf{W}_s^{\mathrm{T}}\mathbf{W}_s\right)^{-1} = \left[\frac{\boldsymbol{S}_{t,1}}{\left(\boldsymbol{S}_{t,1}\right)^{\mathrm{T}}\boldsymbol{S}_{w,1}}\ \cdots\ \frac{\boldsymbol{S}_{t,j}}{\left(\boldsymbol{S}_{t,j}\right)^{\mathrm{T}}\boldsymbol{S}_{w,j}}\right] \tag{41a}$$

$$\mathbf{T}_{\mathrm{B}} = \mathbf{W}_c\left(\mathbf{W}_c^{\mathrm{T}}\mathbf{W}_c\right)^{-1} = \left[\frac{\boldsymbol{S}^*_{t,1}}{\left(\boldsymbol{S}^*_{t,1}\right)^{\mathrm{T}}\boldsymbol{S}^*_{w,1}}\ \cdots\ \frac{\boldsymbol{S}^*_{t,6-j}}{\left(\boldsymbol{S}^*_{t,6-j}\right)^{\mathrm{T}}\boldsymbol{S}^*_{w,6-j}}\right] \tag{41b}$$

Thus, the repelling screw system, namely the twist space of springs and constraints can be written as

$$\mathbf{T} = [\mathbf{T}_s\quad \mathbf{T}_c] = \left(\mathbf{W}^{\mathrm{T}}\right)^{-1}\boldsymbol{\Lambda}_t\left[\mathbf{W}_s\left(\mathbf{W}_s^{\mathrm{T}}\mathbf{W}_s\right)^{-1}\ \mathbf{W}_c\left(\mathbf{W}_c^{\mathrm{T}}\mathbf{W}_c\right)^{-1}\right]\boldsymbol{\Lambda}_t \tag{42a}$$

$$\mathbf{T}_s = \mathbf{T}_{\mathrm{A}}\boldsymbol{\Lambda}_{t,s} = \mathbf{W}_s\left(\mathbf{W}_s^{\mathrm{T}}\mathbf{W}_s\right)^{-1}\boldsymbol{\Lambda}_{t,s} \tag{42b}$$

$$\mathbf{T}_c = \mathbf{T}_{\mathrm{B}}\boldsymbol{\Lambda}_{t,c} = \mathbf{W}_c\left(\mathbf{W}_c^{\mathrm{T}}\mathbf{W}_c\right)^{-1}\boldsymbol{\Lambda}_{t,c} \tag{42c}$$

Note that, as there does not exist displacement along the constraint link, the value of $\delta\theta^*_k$ is always equal to zero. Accordingly, the twist of the rigid platform can be represented as

$$\$_t = \mathbf{T}_s\left(\boldsymbol{\Lambda}_{t,s}\right)^{-1}\delta\boldsymbol{\theta}_s = \ \mathbf{W}_s\left(\mathbf{W}_s^{\mathrm{T}}\mathbf{W}_s\right)^{-1}\delta\boldsymbol{\theta}_s \tag{43}$$

with $\delta\boldsymbol{\theta}_s = [\delta\theta_1\ \cdots\ \delta\theta_j]^{\mathrm{T}}$.

According to Eqs. (41) and (42), $\mathbf{T}_s$ and $\mathbf{T}_c$ are determinated by $\mathbf{T}_{\mathrm{A}}$ and $\mathbf{T}_{\mathrm{B}}$, respectively. From Eq. (40), we can conclude that $\mathbf{W}_c$ has no effect on $\mathbf{T}_s$, and $\mathbf{W}_s$ does not affect $\mathbf{T}_c$. In this situation, we can conclude that $\mathbb{T}_s = \mathbb{W}^*_s$, $\mathbb{T}_c = \mathbb{W}^*_c$. For this special case, the relationships among twist and wrench subspaces of a parallel compliant mechanism are shown in Fig. 4.

4.3. Kinematics and statics of compliant serial mechanisms

4.3.1. Kinematics and statics of general serial compliant mechanisms

For serial compliant mechanisms, a natural choice is to use the unit screws of the compliant joints as the basis elements of $\mathbf{T}_s$. Without consideration of the compliance of constraints, the infinitesimal motion of the mechanism $\$_t$ is only spanned by the elements of $\mathbf{T}_s$. Note that, each element in $\mathbf{T}_s$ is only determined by the position and orientation of its corresponding compliant joint. For the twist space of constraints $\mathbb{T}_c$, we can freely choose any unit screw that is linearly independent with the elements of $\mathbf{T}_s$ to form it basis $\mathbf{T}_c$. By utilizing the duality principle, the relation between the infinitesimal motion and force is given as [44]

$$\$_t = \mathbf{T}\delta\boldsymbol{\theta} \tag{44a}$$

$$\$_w = \left(\mathbf{T}^{\mathrm{T}}\right)^{-1}\delta\boldsymbol{f} \tag{44b}$$

with $\mathbf{T} = [\mathbf{T}_s\ \mathbf{T}_c]$.

Similar to obtaining Eq. (33), the inverse of the transpose of $\mathbf{W}$ can be represented as

$$\left(\mathbf{T}^{\mathrm{T}}\right)^{-1} = [\mathbf{W}_{\mathrm{A}}\ \mathbf{W}_{\mathrm{B}}] = \left[\mathbf{T}_s\mathbf{D}_1^{-1} - \mathbf{T}_c\mathbf{D}_2^{-1}\mathbf{T}_c^{\mathrm{T}}\mathbf{T}_s\left(\mathbf{T}_s^{\mathrm{T}}\mathbf{T}_s\right)^{-1} \quad \mathbf{T}_c\mathbf{D}_2^{-1} - \mathbf{T}_s\left(\mathbf{T}_s^{\mathrm{T}}\mathbf{T}_s\right)^{-1}\mathbf{T}_s^{\mathrm{T}}\mathbf{T}_c\mathbf{D}_2^{-1}\right] \tag{45}$$

Thus

$$\mathbf{W}_{\mathrm{A}} = \mathbf{T}_s\mathbf{D}_1^{-1} - \mathbf{T}_c\mathbf{D}_2^{-1}\mathbf{T}_c^{\mathrm{T}}\mathbf{T}_s\left(\mathbf{T}_s^{\mathrm{T}}\mathbf{T}_s\right)^{-1} \tag{46a}$$

$$\mathbf{W}_{\mathrm{B}} = \mathbf{T}_c\mathbf{D}_2^{-1} - \mathbf{T}_s\left(\mathbf{T}_s^{\mathrm{T}}\mathbf{T}_s\right)^{-1}\mathbf{T}_s^{\mathrm{T}}\mathbf{T}_c\mathbf{D}_2^{-1} \tag{46b}$$

where

$$\mathbf{D}_1 = \left(\mathbf{T}_s^{\mathrm{T}}\mathbf{T}_s - \mathbf{T}_s^{\mathrm{T}}\mathbf{T}_c\left(\mathbf{T}_c^{\mathrm{T}}\mathbf{T}_c\right)^{-1}\mathbf{T}_c^{\mathrm{T}}\mathbf{T}_s\right)$$

$$\mathbf{D}_2 = \left(\mathbf{T}_c^{\mathrm{T}}\mathbf{T}_c - \mathbf{T}_c^{\mathrm{T}}\mathbf{T}_s\left(\mathbf{T}_s^{\mathrm{T}}\mathbf{T}_s\right)^{-1}\mathbf{T}_s^{\mathrm{T}}\mathbf{T}_c\right).$$

Subsequently, we move to the calculation of the repelling screws $\boldsymbol{S}_{w,i}$ $(i=1,\ 2,\ \cdots j)$ and $\boldsymbol{S}^*_{w,k}$ $(k=1,\ 2,\ \cdots 6-j)$ for $\boldsymbol{S}_{t,i}$ $(i=1,\ 2,\ \cdots j)$ and $\boldsymbol{S}^*_{t,k}$ $(k=1,\ 2,\ \cdots 6-j)$. According to Eq. (20), we have

$$\mathbf{W}_{\mathrm{A}} = \left[\frac{\boldsymbol{S}_{w,1}}{\left(\boldsymbol{S}_{w,1}\right)^{\mathrm{T}}\boldsymbol{S}_{t,1}} \cdots \frac{\boldsymbol{S}_{w,j}}{\left(\boldsymbol{S}_{w,j}\right)^{\mathrm{T}}\boldsymbol{S}_{t,j}}\right] \tag{47a}$$

$$\mathbf{W}_{\mathrm{B}} = \left[\frac{\boldsymbol{S}^*_{w,1}}{\left(\boldsymbol{S}^*_{w,1}\right)^{\mathrm{T}}\boldsymbol{S}^*_{t,1}} \cdots \frac{\boldsymbol{S}^*_{w,6-j}}{\left(\boldsymbol{S}^*_{w,6-j}\right)^{\mathrm{T}}\boldsymbol{S}^*_{t,6-j}}\right] \tag{47b}$$

Thus, the repelling screw system, namely the twist space of springs and constraints can be written as

$$\mathbf{W} = [\mathbf{W}_s \quad \mathbf{W}_c] = \left(\mathbf{T}^{\mathrm{T}}\right)^{-1}\boldsymbol{\Lambda}_w \tag{48a}$$

$$\mathbf{W}_s = \mathbf{W}_{\mathrm{A}}\boldsymbol{\Lambda}_{w,s} \tag{48b}$$

$$\mathbf{W}_c = \mathbf{W}_{\mathrm{B}}\boldsymbol{\Lambda}_{w,c} \tag{48c}$$

where

$$\boldsymbol{\Lambda}_w = \mathrm{diag}\left[\left(\boldsymbol{S}_{w,1}\right)^{\mathrm{T}}\boldsymbol{S}_{t,1} \cdots \left(\boldsymbol{S}_{w,j}\right)^{\mathrm{T}}\boldsymbol{S}_{t,j}\ \left(\boldsymbol{S}^*_{w,1}\right)^{\mathrm{T}}\boldsymbol{S}^*_{t,1} \cdots \left(\boldsymbol{S}^*_{w,6-j}\right)^{\mathrm{T}}\boldsymbol{S}^*_{t,6-j}\right]$$

$$\boldsymbol{\Lambda}_{w,s} = \mathrm{diag}\left[\left(\boldsymbol{S}_{w,1}\right)^{\mathrm{T}}\boldsymbol{S}_{t,1} \cdots \left(\boldsymbol{S}_{w,j}\right)^{\mathrm{T}}\boldsymbol{S}_{t,j}\right]$$

$$\boldsymbol{\Lambda}_{w,c} = \mathrm{diag}\left[\left(\boldsymbol{S}^*_{w,1}\right)^{\mathrm{T}}\boldsymbol{S}^*_{t,1} \cdots \left(\boldsymbol{S}^*_{w,6-j}\right)^{\mathrm{T}}\boldsymbol{S}^*_{t,6-j}\right].$$

The physical meaning behind the repelling screw $\boldsymbol{S}_{w,i}$ or $\boldsymbol{S}^*_{w,i}$ can be interpreted as that the force/torque associated with the ith twist of spring (constraint) leads to the force/torque related to the wrence $\boldsymbol{S}_{w,i}$ $(\boldsymbol{S}^*_{w,i})$.

According to Eqs. (47) and (48), $\mathbf{W}_s$ and $\mathbf{W}_c$ can be interpreted as the normalized form of $\mathbf{W}_{\mathrm{A}}$ and $\mathbf{W}_{\mathrm{B}}$, respectively. From Eq. (46), we can conclude that $\mathbf{T}_c$ has effect on $\mathbf{W}_s$, and the change of $\mathbf{T}_s$ leads to the change of $\mathbf{W}_c$. The choice of the basis elements of $\mathbf{T}_c$ affects

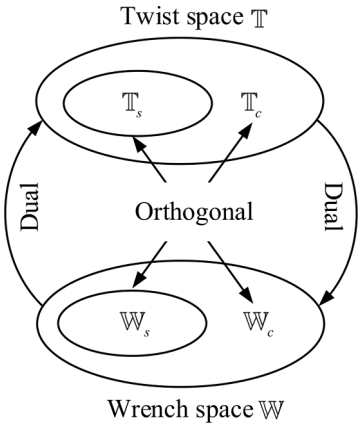

Fig. 5. Relations among twist/wrench spaces, and their subspaces of general compliant serial mechanisms.

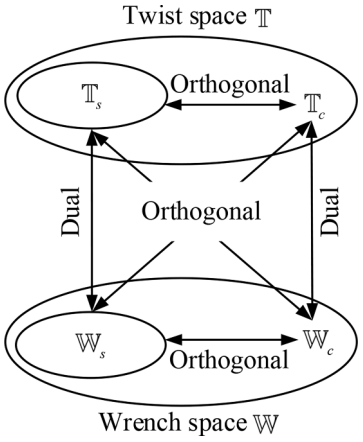

Fig. 6. Relations among twist/wrench spaces, and their subspaces of the serial compliant mechanism when the twist/wrench subspaces of springs are orthogonal to that of constraints.

the wrench space of springs, as well as $\delta \boldsymbol{f}$. Thus the conclusion that $\mathbb{T}_s$ ($\mathbb{T}_c$) and $\mathbb{W}_s$ ($\mathbb{W}_c$) are dual to each other is weakling. The relationships among the twist/wrench subspaces of the general compliant serial mechanism are depicted in Fig. 5.

4.3.2. Orthogonal twist/wrench subspaces of constraints and springs - A Special case for serial configuration

In analogy to the case in Section 4.2.2, there is also a special case, in which $\mathbb{T}_s$ is an orthogonal complement of $\mathbb{T}_c$, and $\mathbb{W}_s$ is an orthogonal complement of $\mathbb{W}_c$. The relations between the subspaces of the twist and wrench of serial compliant mechanism are shown in Fig. 6. According to Eqs. (22)–(24), $\mathbf{T}_c$ can be determinated by the basis elements of Null($\mathbf{T}_s^{\mathrm{T}}$), thus $\boldsymbol{S}_t^*$, namely the element of $\mathbb{T}_c$, belongs to the null space of $\mathbf{T}_s^{\mathrm{T}}$.

The inverse of the transpose of $\mathbf{T}$ can be represented as

$$\left(\mathbf{T}^{\mathrm{T}}\right)^{-1} = [\mathbf{W}_{\mathrm{A}}\ \mathbf{W}_{\mathrm{B}}] = \mathbf{T}\left(\mathbf{T}^{\mathrm{T}}\mathbf{T}\right)^{-1} = [\mathbf{T}_s\ \mathbf{T}_c]\left(\begin{bmatrix}\mathbf{T}_s^{\mathrm{T}}\\ \mathbf{T}_c^{\mathrm{T}}\end{bmatrix}[\mathbf{T}_s\ \mathbf{T}_c]\right)^{-1} = [\mathbf{T}_s\ \mathbf{T}_c]\begin{bmatrix}\mathbf{T}_s^{\mathrm{T}}\mathbf{T}_s & \mathbf{T}_s^{\mathrm{T}}\mathbf{T}_c\\ \mathbf{T}_c^{\mathrm{T}}\mathbf{T}_s & \mathbf{T}_c^{\mathrm{T}}\mathbf{T}_c\end{bmatrix}^{-1} \tag{49}$$

Providing that $\mathbf{T}_s^{\mathrm{T}}\mathbf{T}_c = \mathbf{T}_c^{\mathrm{T}}\mathbf{T}_s = 0$, it can be further written as

$$\left(\mathbf{T}^{\mathrm{T}}\right)^{-1} = [\mathbf{T}_s\ \mathbf{T}_c]\begin{bmatrix}\mathbf{T}_s^{\mathrm{T}}\mathbf{T}_s & \mathbf{0}\\ \mathbf{0} & \mathbf{T}_c^{\mathrm{T}}\mathbf{T}_c\end{bmatrix}^{-1} = \left[\mathbf{T}_s\left(\mathbf{T}_s^{\mathrm{T}}\mathbf{T}_s\right)^{-1}\ \mathbf{T}_c\left(\mathbf{T}_c^{\mathrm{T}}\mathbf{T}_c\right)^{-1}\right] \tag{50}$$

Thus

$$\mathbf{W}_{\mathrm{A}} = \mathbf{T}_s\left(\mathbf{T}_s^{\mathrm{T}}\mathbf{T}_s\right)^{-1} \tag{51a}$$

$$\mathbf{W}_{\mathrm{B}} = \mathbf{T}_c\left(\mathbf{T}_c^{\mathrm{T}}\mathbf{T}_c\right)^{-1} \tag{51b}$$

According to Eq. (27), $\mathbf{W}_{\mathrm{A}}$ and $\mathbf{W}_{\mathrm{B}}$ can be rewritten as

$$\mathbf{W}_{\mathrm{A}} = \mathbf{T}_s\left(\mathbf{T}_s^{\mathrm{T}}\mathbf{T}_s\right)^{-1} = \left[\frac{\boldsymbol{S}_{w,1}}{\left(\boldsymbol{S}_{w,1}\right)^{\mathrm{T}}\boldsymbol{S}_{t,1}} \cdots \frac{\boldsymbol{S}_{w,j}}{\left(\boldsymbol{S}_{w,j}\right)^{\mathrm{T}}\boldsymbol{S}_{t,j}}\right] \tag{52a}$$

$$\mathbf{W}_{\mathrm{B}} = \mathbf{T}_c\left(\mathbf{T}_c^{\mathrm{T}}\mathbf{T}_c\right)^{-1} = \left[\frac{\boldsymbol{S}^*_{w,1}}{\left(\boldsymbol{S}^*_{w,1}\right)^{\mathrm{T}}\boldsymbol{S}^*_{t,1}} \cdots \frac{\boldsymbol{S}^*_{w,6-j}}{\left(\boldsymbol{S}^*_{w,6-j}\right)^{\mathrm{T}}\boldsymbol{S}^*_{t,6-j}}\right] \tag{52b}$$

The repelling screw system, namely the wrench space of springs and constraints with respect to $\boldsymbol{S}_{t,i}$ $(i = 1,\ 2,\ \cdots j)$ and $\boldsymbol{S}^*_{t,k}$ $(k = 1,\ 2,\ \cdots 6-j)$ can be represented as

$$\mathbf{W} = \left(\mathbf{T}^{\mathrm{T}}\right)^{-1}\boldsymbol{\Lambda}_w = \left[\mathbf{T}_s\left(\mathbf{T}_s^{\mathrm{T}}\mathbf{T}_s\right)^{-1}\ \mathbf{T}_c\left(\mathbf{T}_c^{\mathrm{T}}\mathbf{T}_c\right)^{-1}\right]\boldsymbol{\Lambda}_w \tag{53a}$$

$$\mathbf{W}_s = \mathbf{W}_{\mathrm{A}}\boldsymbol{\Lambda}_{w,s} = \mathbf{T}_s\left(\mathbf{T}_s^{\mathrm{T}}\mathbf{T}_s\right)^{-1}\boldsymbol{\Lambda}_{w,s} \tag{53b}$$

$$\mathbf{W}_c = \mathbf{W}_{\mathrm{B}}\boldsymbol{\Lambda}_{w,c} = \mathbf{T}_c\left(\mathbf{T}_c^{\mathrm{T}}\mathbf{T}_c\right)^{-1}\boldsymbol{\Lambda}_{w,c} \tag{53c}$$

According to Eqs. (52) and (53), $\mathbf{W}_s$ and $\mathbf{W}_c$ can be interpreted as the normalized form of $\mathbf{W}_{\mathrm{A}}$ and $\mathbf{W}_{\mathrm{B}}$, respectively. From Eq. (51), we can conclude that $\mathbf{T}_c$ has no effect on $\mathbf{W}_s$. The arrangement of constraints does not affect the twist space of springs. In this situation, $\mathbb{T}_s$ ($\mathbb{T}_c$) and $\mathbb{W}_s$ ($\mathbb{W}_c$) are dual to each other.

4.4. Actuation arrangement based on repelling screws

The repelling screw system can be used for actuation placement in a compliant mechanism. When utilizing force-based actuation [41], any actuation wrench of a compliant mechanism is always linearly independent of its constraint wrenches [42]. For a compliant parallel mechanism, the basis matrix $\mathbf{W}_c$ of its wrench space of constraints can be readily obtained, we can freely choose j unit wrenches that are linearly independent to the basis elements of $\mathbf{W}_c$ to form the basis matrix $\mathbf{W}_a$ of its wrench space of actuators. However, some wrench spaces of actuators may cause relatively large errors due to the compliance of constraints. To overcome this problem, the wrench space of actuators can be determinated as the null space of $\mathbf{W}_c^{\mathrm{T}}$. Preferably, the actuation wrenches of a compliant parallel mechanism have one-to-one correspondence with the basis elements of its freedom space [41] by employing the repelling screw system, thus maximizing the decoupling of force inputs. For a compliant serial mechanism, the determination of its wrench space of actuators is more complicated than that of a compliant parallel mechanism, as the basis matrix $\mathbf{W}_c$ of its wrench space of constraints cannot be obtained from observation. The basis matrix $\mathbf{T}_c$ of a compliant serial mechanism can be determinated as the basis matrix of the null space of $\mathbf{T}_s^{\mathrm{T}}$. Subsequently, the basis matrix $\mathbf{W}_c$ of its wrench space of constraints can be obtained by calculating its repelling screw system with Eq. (53c). Similarly, the wrench space of actuators can be determinated as $\mathrm{Null}(\mathbf{W}_c^{\mathrm{T}})$.

By employing shape-memory-alloy (SMA) springs, a single-DOF flexible element that resists the translation along its axis can be transformed into a linear actuator that generates a stroke along its axis [74]. When actuating the compliant parallel mechanism with SMA actuators, the basis matrix $\mathbf{W}_a$ is the same as $\mathbf{W}_s$, which is obtained by calculating the repelling screw system of the basis matrix $\mathbf{T} = [\mathbf{T}_s\ \mathbf{T}_c]$, where $\mathbf{T}_s$ is determinated by the basis elements of the desired freedom space, and $\mathbf{T}_c$ is obtained by calculating the repelling screw system with Eq. (42c). Thus, each basis element of the desired freedom space corresponds to a specific SMA actuator, and this repelling-screw-based method can be used to maximize the decoupling of actuator inputs. Note that, the detailed analysis of actuation arrangement needs to consider the overall elastic behaviors of a compliant mechanism and the types of actuators, which calls for future study.

5. Configuration transformation between serial and parallel compliant mechanisms

Based the dual and orthogonal properties of compliant mechanisms presented in the proceeding section, the dualities between the stiffness and compliance, as well as parallel and serial configurations are further investigated. From the perspective of repelling screws, an approach for configuration transformation between serial and parallel compliant mechanisms is proposed. Three examples are included to demonstrate the application of this approach.

5.1. Parallel-to-serial transformation of compliant mechanisms

5.1.1. Stiffness inverse of general compliant parallel mechanism

For a spatial parallel complaint mechanism, its stiffness matrix can be written as

$$\mathbf{K} = \mathbf{W}\mathbf{K}_{\theta}\mathbf{W}^{\mathrm{T}} = \boldsymbol{S}_{w,1}k_1\boldsymbol{S}_{w,1}^{\mathrm{T}} + \cdots + \boldsymbol{S}_{w,j}k_j\boldsymbol{S}_{w,j}^{\mathrm{T}} + \boldsymbol{S}^*_{w,1}k^*_1\boldsymbol{S}^{*\mathrm{T}}_{w,1} + \cdots + \boldsymbol{S}^*_{w,6-j}k^*_{6-j}\boldsymbol{S}^{*\mathrm{T}}_{w,6-j} \tag{54}$$

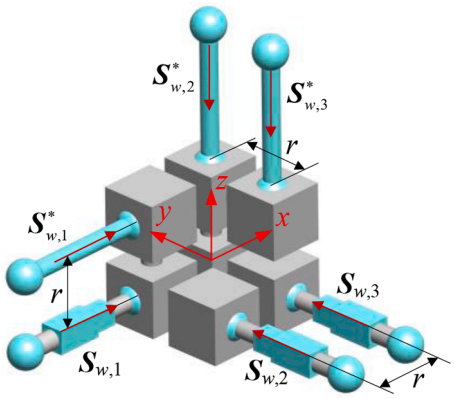

Fig. 7. The spatial compliant parallel platform.

with

$$\mathbf{K}_\theta = \mathrm{diag}\left[k_1 \ \cdots \ k_j \ k_1^* \ \cdots \ k_{6-j}^*\right] \tag{55}$$

where $\mathbf{K}_\theta$ is the joint stiffness matrix of the mechanism. Matrix $\mathbf{K}_\theta$ is usually treated as a constant diagonal matrix, and $k_i^* \to \infty$ $(i = 1, 2, \cdots, 6-j)$, if the constraints are considered rigid.

According to Eq. (35), we have

$$\mathbf{W}^{-T} = \left(\mathbf{W}^{\mathrm{T}}\right)^{-1} = [\,\mathbf{T}_A \quad \mathbf{T}_B\,] = \left[\frac{\boldsymbol{S}_{t,1}}{\left(\boldsymbol{S}_{t,1}\right)^{\mathrm{T}}\boldsymbol{S}_{w,1}} \ \cdots \ \frac{\boldsymbol{S}_{t,j}}{\left(\boldsymbol{S}_{t,j}\right)^{\mathrm{T}}\boldsymbol{S}_{w,j}} \quad \frac{\boldsymbol{S}^*_{t,1}}{\left(\boldsymbol{S}^*_{t,1}\right)^{\mathrm{T}}\boldsymbol{S}^*_{w,1}} \ \cdots \ \frac{\boldsymbol{S}^*_{t,6-j}}{\left(\boldsymbol{S}^*_{t,6-j}\right)^{\mathrm{T}}\boldsymbol{S}^*_{w,6-j}}\right] \tag{56}$$

Thus the inverse of the stiffness matrix can be written in the form of a compliance matrix as

$$\mathbf{C} = \mathbf{K}^{-1} = \left(\mathbf{W}\mathbf{K}_\theta\mathbf{W}^{\mathrm{T}}\right)^{-1} = \mathbf{W}^{-T}\mathbf{K}_\theta^{-1}\mathbf{W}^{-1} = \mathbf{T}\Lambda_t^{-1}\mathbf{K}_\theta^{-1}\boldsymbol{\Lambda}_t^{-1}\mathbf{T}^{\mathrm{T}} = \mathbf{T}\mathbf{C}_\theta\mathbf{T}^{\mathrm{T}} \tag{57}$$

where $\mathbf{C}_\theta$ is the joint compliance matrix of the mechanism. Matrix $\mathbf{C}_\theta$ is usually treated as a constant diagonal matrix, and can be represented as

$$\mathbf{C}_\theta = \boldsymbol{\Lambda}_t^{-1}\mathbf{K}_\theta^{-1}\boldsymbol{\Lambda}_t^{-1} = \mathrm{diag}\left[\frac{1}{k_1\left[\left(\boldsymbol{S}_{t,1}\right)^{\mathrm{T}}\boldsymbol{S}_{w,1}\right]^2} \ \cdots \ \frac{1}{k_j\left[\left(\boldsymbol{S}_{t,j}\right)^{\mathrm{T}}\boldsymbol{S}_{w,j}\right]^2} \quad \frac{1}{k_1^*\left[\left(\boldsymbol{S}^*_{t,1}\right)^{\mathrm{T}}\boldsymbol{S}^*_{w,1}\right]^2} \ \cdots \ \frac{1}{k^*_{6-f}\left[\left(\boldsymbol{S}^*_{t,6-j}\right)^{\mathrm{T}}\boldsymbol{S}^*_{w,6-j}\right]^2}\right] \tag{58}$$

As $\frac{1}{k_i^*} \to 0$, Eq. (58) can be rewritten as

$$\mathbf{C} = \mathbf{T}_s\boldsymbol{\Lambda}_{t,s}^{-1}\mathbf{K}_{\theta,s}^{-1}\boldsymbol{\Lambda}_{t,s}^{-1}\mathbf{T}_s^{\mathrm{T}} = \mathbf{T}_s\mathbf{C}_{\theta,s}\mathbf{T}_s^{\mathrm{T}} \tag{59}$$

where

$$\mathbf{K}_{\theta,s} = \mathrm{diag}[\,k_1 \quad \cdots \quad k_j\,] \tag{60a}$$

$$\mathbf{C}_{\theta,s} = \boldsymbol{\Lambda}_{t,s}^{-1}\mathbf{K}_{\theta,s}^{-1}\boldsymbol{\Lambda}_{t,s}^{-1} = \mathrm{diag}\left[\frac{1}{k_1\left[\left(\boldsymbol{S}_{t,1}\right)^{\mathrm{T}}\boldsymbol{S}_{w,1}\right]^2} \quad \cdots \quad \frac{1}{k_j\left[\left(\boldsymbol{S}_{t,j}\right)^{\mathrm{T}}\boldsymbol{S}_{w,j}\right]^2}\right] \tag{60b}$$

Thus the stiffness matrix developed in Eq. (54) can be constructed using an equivalent serial mechanism whose joints are associated with repelling screws $\boldsymbol{S}_{t,i}$ $(i = 1, 2, \cdots, j)$. The relationship between the six wrenches, namely $\boldsymbol{S}_{w,i}$ $(i = 1, 2, \cdots, 6)$ of a compliant parallel mechanism, and their repelling screws, namely the six twists $\boldsymbol{S}_{t,i}$ $(i = 1, 2, \cdots, 6)$ of an equivalent compliant serial mechanism, has been previously identified in [18], and was explained as that a nonzero wrench/twist cannot be reciprocal to six independent twists/wrenches, thus can be uniquely determined by five independent twists/wrenches. It is noticed in general $\boldsymbol{S}_{t,i}$ and $\boldsymbol{S}^*_{w,i}$ may not have zero pitches, thus a screw-type joint or constraint can be adopted to represent it [75,76].

5.1.2. Examples 1 and 2: parallel-to-serial transformation

In this section, two examples of parallel-to-serial transformation are presented and illustrated. Example 1 is related to the general case of compliant parallel mechanism introduced in Section 4.2.1, and Example 2 corresponds to the special case of compliant parallel

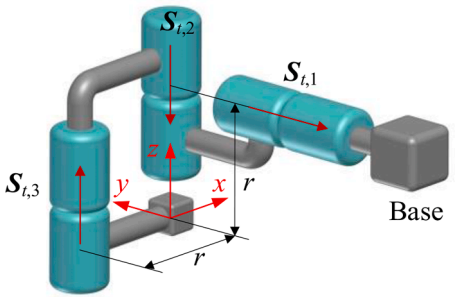

Fig. 8. The corresponding compliant serial platform.

mechanism, in which the twist/wrench subspaces of springs are orthogonal to that of constraints, as introduced in Section 4.2.2.

- **Example 1:** General compliant parallel mechanism

For a compliant parallel mechanism, its basis of wrench space has the form as

$$\begin{aligned}\mathbf{W} &= [\,\mathbf{W}_s \quad \mathbf{W}_c\,] = \begin{bmatrix} \boldsymbol{S}_{w,1} & \boldsymbol{S}_{w,2} & \boldsymbol{S}_{w,3} & \boldsymbol{S}^*_{w,1} & \boldsymbol{S}^*_{w,2} & \boldsymbol{S}^*_{w,3} \end{bmatrix} \\ &= \begin{bmatrix} 1 & 0 & 0 & 1 & 0 & 0 \\ 0 & 1 & 1 & 0 & 0 & 0 \\ 0 & 0 & 0 & 0 & -1 & -1 \\ 0 & 0 & 0 & 0 & 0 & r \\ 0 & 0 & 0 & r & 0 & 0 \\ 0 & -r & 0 & 0 & 0 & 0 \end{bmatrix}\end{aligned} \tag{61}$$

For the limb with spring, it is a compliant prismatic joint with linear stiffness k_i $(i = 1,\ 2,\ 3)$. The constraint limb is a rigid link with linear stiffness k^*_j $(j = 1,\ 2,\ 3)$. The schematic diagram of this compliant parallel platform is shown in Fig. 7. The null space of $\mathbf{W}_s^{\mathrm{T}}$can be expressed as

$$\mathrm{Null}\left(\mathbf{W}_s^{\mathrm{T}}\right) = \mathrm{Span}\left(\boldsymbol{n}_{w,1}, \boldsymbol{n}_{w,2}, \boldsymbol{n}_{w,3}\right) \tag{62}$$

where $\boldsymbol{n}_{w,1} = [0\ \ 0\ \ 1\ \ 0\ \ 0\ \ 0]^{\mathrm{T}}$, $\boldsymbol{n}_{w,2} = [0\ \ 0\ \ 0\ \ 1\ \ 0\ \ 0]^{\mathrm{T}}$, and $\boldsymbol{n}_{w,3} = [0\ \ 0\ \ 0\ \ 0\ \ 1\ \ 0]^{\mathrm{T}}$. It is found that $\boldsymbol{S}^*_{w,1} \notin \mathrm{Null}(\mathbf{W}_s^{\mathrm{T}})$, which means the subspaces $\mathbb{T}_s$ $(\mathbb{W}_s)$ and $\mathbb{T}_c$ $(\mathbb{W}_c)$ are not orthogonal to each other.

Now we turn to the inverse of the stiffness matrix. First the inverse of the transpose of wrench matrix in forms of repelling screws can be written as

$$\begin{aligned}\left(\mathbf{W}^{\mathrm{T}}\right)^{-1} &= \begin{bmatrix} \mathbf{T}_s\boldsymbol{\Lambda}_{t,s}^{-1} & \mathbf{T}_c\boldsymbol{\Lambda}_{t,c}^{-1} \end{bmatrix} = \mathbf{T}\Lambda_t^{-1} \\ &= \begin{bmatrix} r & 0 & 0 & 0 & 0 & 0 \\ 0 & 0 & r & 0 & 0 & 0 \\ 0 & 0 & 0 & 0 & -r & 0 \\ 0 & 0 & 0 & 0 & -1 & 1 \\ -1 & 0 & 0 & 1 & 0 & 0 \\ 0 & -1 & 1 & 0 & 0 & 0 \end{bmatrix} \mathrm{diag}\left[\frac{1}{r} \quad \frac{1}{r} \quad \frac{1}{r} \quad \frac{1}{r} \quad \frac{1}{r} \quad \frac{1}{r}\right]\end{aligned} \tag{63}$$

with $\mathbf{T}_s = [\,\boldsymbol{S}_{t,1} \quad \boldsymbol{S}_{t,2} \quad \boldsymbol{S}_{t,3}\,] = \begin{bmatrix} r & 0 & 0 \\ 0 & 0 & r \\ 0 & 0 & 0 \\ 0 & 0 & 0 \\ -1 & 0 & 0 \\ 0 & -1 & 1 \end{bmatrix}$; $\boldsymbol{\Lambda}_{t,s}^{-1} = \mathrm{diag}\left[\frac{1}{r} \quad \frac{1}{r} \quad \frac{1}{r}\right]$.

According to Eqs. (59) and (60), the compliance matrix is obtained by

$$\mathbf{C} = \mathbf{T}_s\mathbf{C}_{\theta,s}\mathbf{T}_s^{\mathrm{T}} \tag{64}$$

with

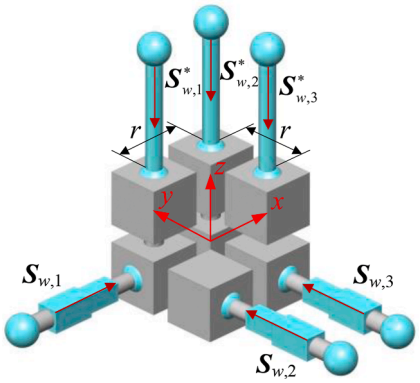

Fig. 9. The compliant parallel platform with orthogonal wrench subspaces, respectively corresponding to compliant and constraint limbs.

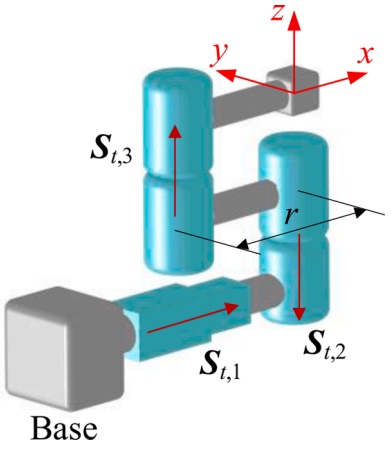

Fig. 10. The corresponding compliant serial platform of the compliant parallel mechanisms with orthogonal subspaces of wrenches.

$$\mathbf{C}_{\theta,s} = \boldsymbol{\Lambda}_{t,s}^{-1}\mathbf{K}_{\theta,s}^{-1}\boldsymbol{\Lambda}_{t,s}^{-1} = \operatorname{diag}\left[\frac{1}{k_1 r^2} \quad \frac{1}{k_2 r^2} \quad \frac{1}{k_3 r^2}\right] \tag{65}$$

It is easy to identify that each repelling screw is associated with a twist that is represented in Plücker axis coordinate frame. The developed compliance matrix is related to a compliant serial mechanism, and the corresponding schematic diagram is depicted in Fig. 8.

- **Example 2:** Compliant parallel mechanism with orthogonal twist/wrench subspaces of constraints and springs

For a compliant parallel mechanism, its basis of wrench space has the form as

$$\begin{aligned}\mathbf{W} = [\mathbf{W}_s \quad \mathbf{W}_c] &= \begin{bmatrix}\boldsymbol{S}_{w,1} & \boldsymbol{S}_{w,2} & \boldsymbol{S}_{w,3} & \boldsymbol{S}^*_{w,1} & \boldsymbol{S}^*_{w,2} & \boldsymbol{S}^*_{w,3}\end{bmatrix} \\ &= \begin{bmatrix} 1 & 0 & 0 & 0 & 0 & 0 \\ 0 & 1 & 1 & 0 & 0 & 0 \\ 0 & 0 & 0 & -1 & -1 & -1 \\ 0 & 0 & 0 & 0 & 0 & r \\ 0 & 0 & 0 & -r & 0 & 0 \\ 0 & -r & 0 & 0 & 0 & 0 \end{bmatrix}\end{aligned} \tag{66}$$

Similar to Example 1, the ith limb with spring i comprises a compliant prismatic joint with linear stiffness k_i $(i = 1,\ 2,\ 3)$, and the constraint limb is a rigid link with linear stiffness k_j^* $(j = 1,\ 2,\ 3)$. The schematic diagram of this compliant parallel platform is shown in Fig. 9. The null space of $\mathbf{W}_s^{\mathrm{T}}$ is identical with that in Example 1. It is easy to see that $\boldsymbol{S}^*_{w,1}$, $\boldsymbol{S}^*_{w,2}$ and $\boldsymbol{S}^*_{w,3} \in \mathrm{Null}(\mathbf{W}_s^{\mathrm{T}})$, which indicates $\mathbb{T}_c$ is an orthocomplement space of $\mathbb{T}_s$. Thus we have

$$\mathbf{T}_A = \mathbf{W}_s\left(\mathbf{W}_s^{\mathrm{T}}\mathbf{W}_s\right)^{-1} = \mathbf{T}_s\boldsymbol{\Lambda}_{t,s}^{-1} = \begin{bmatrix} 1 & 0 & 0 \\ 0 & 0 & r \\ 0 & 0 & 0 \\ 0 & 0 & 0 \\ 0 & 0 & 0 \\ 0 & -1 & 1 \end{bmatrix} \mathrm{diag}\begin{bmatrix} 1 & \frac{1}{r} & \frac{1}{r} \end{bmatrix} \tag{67}$$

with $\mathbf{T}_s = \begin{bmatrix} 1 & 0 & 0 \\ 0 & 0 & r \\ 0 & 0 & 0 \\ 0 & 0 & 0 \\ 0 & 0 & 0 \\ 0 & -1 & 1 \end{bmatrix}$; $\boldsymbol{\Lambda}_{t,s}^{-1} = \mathrm{diag}\begin{bmatrix} 1 & \frac{1}{r} & \frac{1}{r} \end{bmatrix}$.

Accordingly, $\mathbf{C}_{\theta,s}$ can be expressed as

$$\mathbf{C}_{\theta,s} = \boldsymbol{\Lambda}_{t,s}^{-1}\mathbf{K}_{\theta,s}^{-1}\boldsymbol{\Lambda}_{t,s}^{-1} = \mathrm{diag}\begin{bmatrix} \frac{1}{k_1} & \frac{1}{k_2 r^2} & \frac{1}{k_3 r^2} \end{bmatrix} \tag{68}$$

and the compliance matrix can be written as

$$\mathbf{C} = \mathbf{T}_s\mathbf{C}_{\theta,s}\mathbf{T}_s^{\mathrm{T}} \tag{69}$$

The corresponding schematic diagram of this compliant serial platform is shown in Fig. 10.

5.2. Serial-to-parallel transformation of compliant mechanisms

5.2.1. Compliance inverse of compliant parallel mechanism

For a spatial serial complaint mechanism, its compliance matrix can be written as

$$\mathbf{C} = \mathbf{T}\mathbf{C}_\theta\mathbf{T}^{\mathrm{T}} = \boldsymbol{S}_{t,1}c_1\boldsymbol{S}_{t,1}^{\mathrm{T}} + \cdots + \boldsymbol{S}_{t,j}c_j\boldsymbol{S}_{t,j}^{\mathrm{T}} + \boldsymbol{S}_{t,1}^{*}c_1^{*}\boldsymbol{S}_{t,1}^{*\mathrm{T}} + \cdots + \boldsymbol{S}_{t,6-j}^{*}c_{6-j}^{*}\boldsymbol{S}_{t,6-j}^{*\mathrm{T}} \tag{70}$$

where $\mathbf{C}_\theta = \mathrm{diag}[c_1\ \cdots\ c_j\ c_1^{*}\ \cdots\ c_{6-j}^{*}]$ is the joint compliance matrix of the mechanism. Matrix $\mathbf{C}_\theta$ is usually treated as a constant diagonal matrix, and $c_i^{*} \to 0$, $i = 1,\ 2,\ \cdots,\ 6-j$. $\boldsymbol{S}_{t,i}^{*}$ $(i = 1,\ 2,\ \cdots,\ 6-j)$ is linearly independent with $\boldsymbol{S}_{t,i}^{*}$ $(i \neq j)$ and the elements of $\mathbf{T}_s$.

According to Eq. (47), we have

$$\mathbf{T}^{-\mathrm{T}} = \left(\mathbf{T}^{\mathrm{T}}\right)^{-1} = \begin{bmatrix} \mathbf{W}_A & \mathbf{W}_B \end{bmatrix} = \begin{bmatrix} \frac{\boldsymbol{S}_{w,1}}{\left(\boldsymbol{S}_{w,1}\right)^{\mathrm{T}}\boldsymbol{S}_{t,1}} & \cdots & \frac{\boldsymbol{S}_{w,j}}{\left(\boldsymbol{S}_{w,j}\right)^{\mathrm{T}}\boldsymbol{S}_{t,j}} & \frac{\boldsymbol{S}_{w,1}^{*}}{\left(\boldsymbol{S}_{w,1}^{*}\right)^{\mathrm{T}}\boldsymbol{S}_{t,1}^{*}} & \cdots & \frac{\boldsymbol{S}_{w,6-j}^{*}}{\left(\boldsymbol{S}_{w,6-j}^{*}\right)^{\mathrm{T}}\boldsymbol{S}_{t,6-j}^{*}} \end{bmatrix} \tag{71}$$

Thus the inverse of the compliance matrix can be written in the form of stiffness matrix as

$$\mathbf{K} = \mathbf{C}^{-1} = \left(\mathbf{T}\mathbf{C}_\theta\mathbf{T}^{\mathrm{T}}\right)^{-1} = \mathbf{T}^{-T}\mathbf{C}_\theta^{-1}\mathbf{T}^{-1} = \mathbf{W}\Lambda_w^{-1}\mathbf{C}_\theta^{-1}\boldsymbol{\Lambda}_w^{-1}\mathbf{W}^{\mathrm{T}} = \mathbf{W}\mathbf{K}_\theta\mathbf{W}^{\mathrm{T}} \tag{72}$$

where $\mathbf{K}_\theta$ is the joint stiffness matrix of the mechanism. Matrix $\mathbf{K}_\theta$ can be represented as

$$\mathbf{K}_\theta = \boldsymbol{\Lambda}_w^{-1}\mathbf{C}_\theta^{-1}\boldsymbol{\Lambda}_w^{-1} = \mathrm{diag}\left[\frac{1}{c_1\left[\left(\boldsymbol{S}_{w,1}\right)^{\mathrm{T}}\boldsymbol{S}_{t,1}\right]^2} \cdots \frac{1}{c_j\left[\left(\boldsymbol{S}_{w,j}\right)^{\mathrm{T}}\boldsymbol{S}_{t,j}\right]^2} \frac{1}{c_1^{*}\left[\left(\boldsymbol{S}_{w,1}^{*}\right)^{\mathrm{T}}\boldsymbol{S}_{t,1}^{*}\right]^2} \cdots \frac{1}{c_{6-j}^{*}\left[\left(\boldsymbol{S}_{w,6-j}^{*}\right)^{\mathrm{T}}\boldsymbol{S}_{t,6-j}^{*}\right]^2}\right] \tag{73}$$

Eq. (72) can be rewritten as

$$\mathbf{K} = \mathbf{W}_s\boldsymbol{\Lambda}_{w,s}^{-1}\mathbf{C}_{\theta,s}^{-1}\boldsymbol{\Lambda}_{w,s}^{-1}\mathbf{W}_s^{\mathrm{T}} + \mathbf{W}_c\boldsymbol{\Lambda}_{w,c}^{-1}\mathbf{C}_{\theta,c}^{-1}\boldsymbol{\Lambda}_{w,c}^{-1}\mathbf{W}_c^{\mathrm{T}} = \mathbf{W}_s\mathbf{K}_{\theta,s}\mathbf{W}_s^{\mathrm{T}} + \mathbf{W}_c\mathbf{K}_{\theta,c}\mathbf{W}_c^{\mathrm{T}} \tag{74}$$

where

$$\mathbf{C}_{\theta,s} = \mathrm{diag}\left[c_1 \quad \cdots \quad c_j\right] \tag{75a}$$

$$\mathbf{C}_{\theta,c} = \mathrm{diag}\left[c_1^{*} \quad \cdots \quad c_{6-f}^{*}\right] \tag{75b}$$

$$\mathbf{K}_{\theta,s} = \boldsymbol{\Lambda}_{w,s}^{-1}\mathbf{C}_{\theta,s}^{-1}\boldsymbol{\Lambda}_{w,s}^{-1} = \mathrm{diag}\left[\frac{1}{c_1\left[\left(\boldsymbol{S}_{w,1}\right)^{\mathrm{T}}\boldsymbol{S}_{t,1}\right]^2} \quad \cdots \quad \frac{1}{c_j\left[\left(\boldsymbol{S}_{w,j}\right)^{\mathrm{T}}\boldsymbol{S}_{t,j}\right]^2}\right] \tag{75c}$$

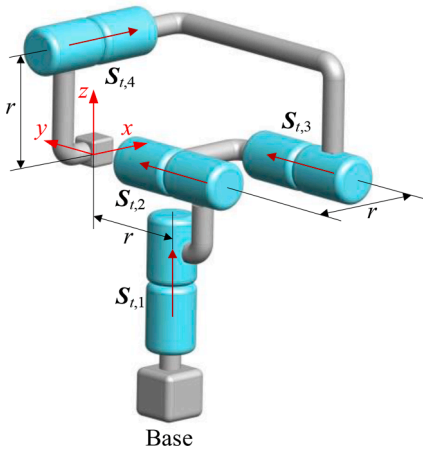

Fig. 11. The spatial compliant serial parallel platform.

$$\mathbf{K}_{\theta,c} = \boldsymbol{\Lambda}_{w,c}^{-1}\mathbf{C}_{\theta,c}^{-1}\boldsymbol{\Lambda}_{w,c}^{-1} = \operatorname{diag}\left[\frac{1}{c_1^*\left[\left(\boldsymbol{S}_{w,1}^*\right)^{\mathrm{T}}\boldsymbol{S}_{t,1}^*\right]^2} \quad \cdots \quad \frac{1}{c_{6-j}^*\left[\left(\boldsymbol{S}_{w,6-j}^*\right)^{\mathrm{T}}\boldsymbol{S}_{t,6-j}^*\right]^2}\right] \tag{75d}$$

As $\frac{1}{c_i^*} \to \infty$, $\mathbf{W}_c\mathbf{K}_{\theta,c}\mathbf{W}_c^{\mathrm{T}}$ corresponds to the stiffness provided by constraints. $\boldsymbol{S}_{w,i}^*$, $i = 1,\ 2,\ \cdots 6-j$ represents the location and orientation of the ith constraint.

Thus the compliance matrix developed in Eq. (70) can be constructed using an equivalent parallel mechanism whose joints and constraints are associated with repelling screws $\boldsymbol{S}_{w,i}$ ($i = 1,\ 2,\ \cdots\cdots j$) and $\boldsymbol{S}_{w,i}^*$ ($i = 1,\ 2,\ \cdots\cdots 6-j$), respectively. It is noticed in general $\boldsymbol{S}_{w,i}$ ($i = 1,\ 2,\ \cdots\cdots j$) / $\boldsymbol{S}_{w,i}^*$ ($i = 1,\ 2,\ \cdots\cdots 6-j$) may not have zero pitches, thus the screw-type joint/constraint can be adopted. The screw-type constraint can be generated by specially designed mechanism.

Note that, different choices of $\boldsymbol{S}_{t,i}^*$ ($i = 1,\ 2,\ \cdots\ldots,\ 6-j$) lead to different compliant parallel mechanism. In addition, if $\boldsymbol{S}_{t,i}^*$ ($i = 1,\ 2,\ \cdots\ldots,\ 6-j$) $\in \mathrm{Null}(\mathbf{T}_s^{\mathrm{T}})$, $\mathbf{T}_c$ does not affect the wrench space $\mathbf{W}$. Thus the overall arrangement of the constraints of the parallel counterpart is adjustable and can be optimized according to the conditions of the installation space.

5.2.2. *Example 3: serial-to-parallel transformation*

As analysed in Section 4.3.1, different choice of the basis elements of $\mathbf{T}_c$ affects the wrench space $\mathbf{W}$, which leads to different configurations of its parallel counterpart. In this section, we look into the special case that the elements of $\mathbf{T}_c$ belongs to $\mathrm{Null}(\mathbf{T}_s^{\mathrm{T}})$.

For a compliant serial mechanism, its Jacobian matrix has the form as

$$\begin{aligned}\mathbf{T}_s &= [\boldsymbol{S}_{t,1} \quad \boldsymbol{S}_{t,2} \quad \boldsymbol{S}_{t,3} \quad \boldsymbol{S}_{t,4}] \\ &= \begin{bmatrix} -r & 0 & 0 & 0 \\ 0 & 0 & 0 & r \\ 0 & 0 & r & 0 \\ 0 & 0 & 0 & 1 \\ 0 & 1 & 1 & 0 \\ 1 & 0 & 0 & 0 \end{bmatrix}\end{aligned} \tag{76}$$

Each twist is associated with a compliant revolute joint with torsional compliance c_i ($i = 1,\ 2,\ 3,\ 4$). The schematic diagram of this compliant parallel mechanism is shown in Fig. 11. The null space of $\mathbf{T}_s^{\mathrm{T}}$ can be expressed as

$$\mathrm{Null}\left(\mathbf{T}_s^{\mathrm{T}}\right) = \mathrm{Span}\left(\boldsymbol{n}_{t,1},\ \boldsymbol{n}_{t,2}\right) \tag{77}$$

where $\boldsymbol{n}_{t,1} = \begin{bmatrix} 0 & -\frac{1}{r} & 0 & 1 & 0 & 0 \end{bmatrix}^{\mathrm{T}}$, and $\boldsymbol{n}_{t,2} = \begin{bmatrix} \frac{1}{r} & 0 & 0 & 0 & 0 & 1 \end{bmatrix}^{\mathrm{T}}$.

We choose $\boldsymbol{S}_{t,1}^*$and $\boldsymbol{S}_{t,2}^*$from $\mathrm{Null}(\mathbf{T}_s^{\mathrm{T}})$ and set $\boldsymbol{S}_{t,1}^* = \boldsymbol{n}_{t,1}$ and $\boldsymbol{S}_{t,2}^* = \boldsymbol{n}_{t,2}$. Thus

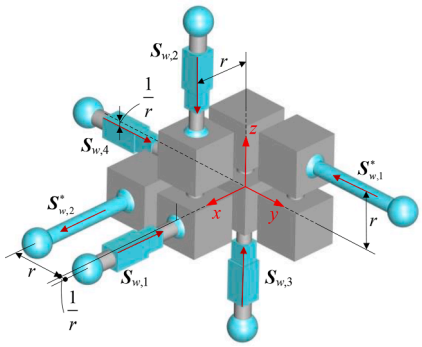

Fig. 12. The corresponding compliant parallel platform ($r = 16$ mm).

$$\mathbf{T} = [\mathbf{T}_s \quad \mathbf{T}_c] = [\boldsymbol{S}_{t,1} \quad \boldsymbol{S}_{t,2} \quad \boldsymbol{S}_{t,3} \quad \boldsymbol{S}_{t,4} \quad \boldsymbol{S}^*_{t,1} \quad \boldsymbol{S}^*_{t,2}]$$
$$= \begin{bmatrix} -r & 0 & 0 & 0 & 0 & \frac{1}{r} \\ 0 & 0 & 0 & r & -\frac{1}{r} & 0 \\ 0 & 0 & r & 0 & 0 & 0 \\ 0 & 0 & 0 & 1 & 1 & 0 \\ 0 & 1 & 1 & 0 & 0 & 0 \\ 1 & 0 & 0 & 0 & 0 & 1 \end{bmatrix} \tag{78}$$

Now we turn to the inverse of the compliance matrix. First the inverse of the transpose of twist matrix in the form of repelling screws can be written as

$$(\mathbf{T}^{\mathrm{T}})^{-1} = \begin{bmatrix} \mathbf{W}_s \boldsymbol{\Lambda}^{-1}_{w,s} & \mathbf{W}_c \boldsymbol{\Lambda}^{-1}_{w,c} \end{bmatrix} = \mathbf{W} \Lambda^{-1}_w$$
$$= \begin{bmatrix} -1 & 0 & 0 & 0 & 0 & 1 \\ 0 & 0 & 0 & 1 & -1 & 0 \\ 0 & -1 & 1 & 0 & 0 & 0 \\ 0 & 0 & 0 & \frac{1}{r} & r & 0 \\ 0 & r & 0 & 0 & 0 & 0 \\ \frac{1}{r} & 0 & 0 & 0 & 0 & r \end{bmatrix} \mathrm{diag}\left[\frac{r}{r^2+1} \quad \frac{1}{r} \quad \frac{1}{r} \quad \frac{r}{r^2+1} \quad \frac{r}{r^2+1} \quad \frac{r}{r^2+1}\right] \tag{79}$$

with $\mathbf{W}_s = \begin{bmatrix} -1 & 0 & 0 & 0 \\ 0 & 0 & 0 & 1 \\ 0 & -1 & 1 & 0 \\ 0 & 0 & 0 & \frac{1}{r} \\ 0 & r & 0 & 0 \\ \frac{1}{r} & 0 & 0 & 0 \end{bmatrix}$; $\boldsymbol{\Lambda}^{-1}_{w,s} = \mathrm{diag}\left[\frac{r}{r^2+1} \quad \frac{1}{r} \quad \frac{1}{r} \quad \frac{r}{r^2+1}\right]$; $\mathbf{W}_c = \begin{bmatrix} 0 & 1 \\ -1 & 0 \\ 0 & 0 \\ r & 0 \\ 0 & 0 \\ 0 & r \end{bmatrix}$; $\boldsymbol{\Lambda}^{-1}_{w,c} = \mathrm{diag}\left[\frac{r}{r^2+1} \quad \frac{r}{r^2+1}\right]$.

According to Eqs. (74) and (75), the 6 × 6 stiffness matrix is obtained by

$$\mathbf{K} = \mathbf{W}_s \mathbf{K}_{\theta,s} \mathbf{W}_s^{\mathrm{T}} + \mathbf{W}_c \mathbf{K}_{\theta,c} \mathbf{W}_c^{\mathrm{T}} \tag{80}$$

with

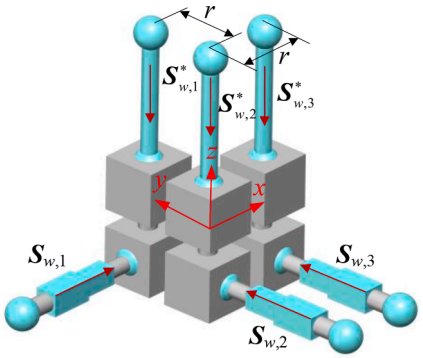

Fig. 13. An equivalent compliant parallel mechanism of the mechanism in Example 2 (Fig. 9).

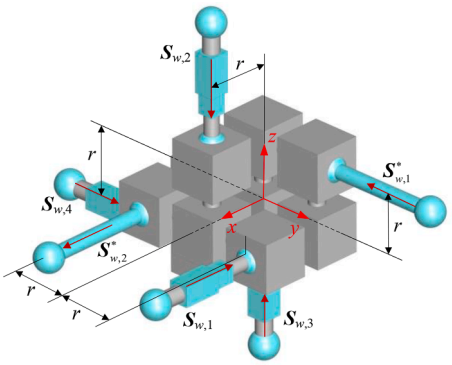

Fig. 14. An equivalent compliant parallel mechanism of the mechanism in Example 3 (Fig. 12).

$$\mathbf{K}_{\theta,s} = \boldsymbol{\Lambda}_{w,s}^{-1}\mathbf{C}_{\theta,s}^{-1}\boldsymbol{\Lambda}_{w,s}^{-1} = \operatorname{diag}\left[\frac{r^2}{c_1\left(r^2+1\right)^2} \quad \frac{1}{c_2 r^2} \quad \frac{1}{c_3 r^2} \quad \frac{r^2}{c_4\left(r^2+1\right)^2}\right] \tag{81}$$

It is easy to identify that each repelling screw is associated with a wrench that is represented in Plücker ray coordinate frame. The developed stiffness matrix is related to a compliant parallel mechanism, and the corresponding schematic diagram is depicted in Fig. 12 ($r = 16$ mm). In analogy to Example 2 in the Section 5.1.2, when belonging to the null space of $\mathbf{T}_s^{\mathrm{T}}$, the twists of constraint does not affect the Jacobian matrix of its equivalent parallel mechanism.

5.3. Adjustment of the target configuration

5.3.1. Adjustment of the constraint space

Note that, when belonging to the null space of $\mathbf{W}_s^{\mathrm{T}}$, the wrenches of constraint does not affect the configuration of its equivalent serial mechanism. Thus we can choose constraint wrenches that belong to Null($\mathbf{W}_s^{\mathrm{T}}$) to construct the constraint mode so as to change the configuration of the compliant mechanism. Without loss of generality, we take the planar case of Example 2 as an example. The wrench corresponding to the 2th constraint limb of the configuration in Fig. 13 is different from that of the configuration in Fig. 9, while the other constraints and flexible limbs are identical to each other. For the configuration in Fig. 13, $\boldsymbol{S}^*_{w,2} = [0 \quad 0 \quad -1 \quad r \quad -r \quad 0]^T$, and $\boldsymbol{S}^*_{w,2} \in$ Null($\mathbf{W}_s^T$). Its serial counterpart is identical with that of the parallel configuration in Example 2, see Fig. 10.

5.3.2. Adjustment of the dimensional/stiffness parameters

It is noteworthy that a characteristic length L can be defined to normalize the dimensional parameters so as to adjust the target configuration. We take Example 3 as an example. All dimensional parameters are normalized by L, Eq. (79) can be rewritten as

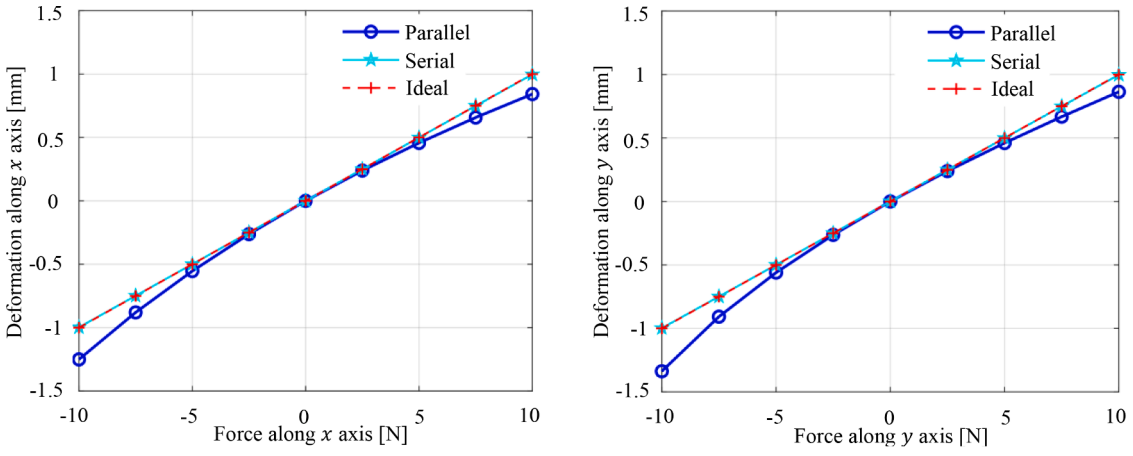

Fig. 15. Deformations of the compliant mechanisms in Example 2 when the force is collinear with (a) x axis, and (b) y axis.

$$\left(\mathbf{T}^{\mathrm{T}}\right)^{-1} = \begin{bmatrix} \mathbf{W}_s\boldsymbol{A}_{w,s}^{-1} & \mathbf{W}_c\boldsymbol{A}_{w,c}^{-1} \end{bmatrix} = \mathbf{W}\Lambda_w^{-1}$$

$$= \begin{bmatrix} -1 & 0 & 0 & 0 & 0 & 1 \\ 0 & 0 & 0 & 1 & -1 & 0 \\ 0 & -1 & 1 & 0 & 0 & 0 \\ 0 & 0 & 0 & \frac{L}{r} & \frac{r}{L} & 0 \\ 0 & \frac{r}{L} & 0 & 0 & 0 & 0 \\ \frac{L}{r} & 0 & 0 & 0 & 0 & \frac{r}{L} \end{bmatrix} \mathrm{diag}\left[\frac{rL}{r^2+L^2} \quad \frac{L}{r} \quad \frac{L}{r} \quad \frac{rL}{r^2+L^2} \quad \frac{rL}{r^2+L^2} \quad \frac{rL}{r^2+L^2} \right] \tag{82}$$

According to Eq. (81), the joint stiffness matrix of the new configuration can be expressed as

$$\mathbf{K}_{\theta,s} = \mathrm{diag}\left[\frac{r^2L^2}{c_1\left(r^2+L^2\right)^2} \quad \frac{L^2}{c_2r^2} \quad \frac{L^2}{c_3r^2} \quad \frac{r^2L^2}{c_4\left(r^2+L^2\right)^2} \right] \tag{83}$$

Thus the characteristic length L also leads to the change of the stiffness parameters of the springs in the new configuration. Fig. 14 illustrates the new configuration when $L = r$ and $r = 16$mm, which has different relative dimensions compared with the configuration in Fig. 12. For this configuration, the joint stiffness matrix $\mathbf{K}_{\theta,s} = \mathrm{diag}\left[\frac{1}{4c_1} \quad \frac{1}{c_2} \quad \frac{1}{c_3} \quad \frac{1}{4c_4} \right]$.

6. Simulation

In this section, the simulation was conducted in ANSYS to validate the proposed duality analysis as well as the approach of configuration transformation. We assume that all components except for the springs are rigid, and the geometric parameter r is set as 16 mm. The simulation results of the three examples in Section 5 are discussed as follows:

6.1. Simulation of Example 1

In this simulation, the stiffness of the three springs in the compliant parallel mechanism is equal to 10 N/mm. With Eq. (65), the stiffness of the three springs in the compliant serial mechanism is 2560 N · mm/rad. When the force is collinear with either x or y axis, the deformations of the compliant mechanisms in both theory and simulation are displayed in Fig. 15. It is found that the elastic behaviors of the compliant serial mechanism are very close to the ideal ones in theory. For the compliant parallel mechanism, the translational stiffnesses along x axis and y axis gain gradually, as the force increases from −10 to 10 N. Note that, the stiffness is indicated as the inverse of the slope of the curve. The mean margins of the stiffness errors along x and y axes are 12.05% and 12.47%, respectively. When the forces increase from −5 to 5 N, the mean margins of the stiffness errors along x and y axes decrease to 7.17% and 7.24%, respectively. Note that, when the forces along x axis and y axis are close to zero, the translational stiffnesses approach to

Table 1
Deformations of the compliant mechanisms in Example 1 when the force (parallel to z axis) is applied on the point $(0,\ 0,\ 0)$ mm.

$\boldsymbol{F}$ imposed on the point $(0,\ 0,\ 0)$mm (N)	Displacement along x axis (mm)		Displacement along y axis (mm)		Displacement along z axis (mm)	
	Parallel	Serial	Parallel	Serial	Parallel	Serial
$[0\ \ 0\ \ -10]^T$	2.40×10^{-7}	1.17×10^{-8}	-9.18×10^{-8}	6.85×10^{-8}	-1.57×10^{-6}	-9.41×10^{-5}
$[0\ \ 0\ \ -5]^T$	1.24×10^{-7}	6.07×10^{-9}	-3.41×10^{-8}	3.42×10^{-8}	-7.87×10^{-7}	-4.70×10^{-5}
$[0\ \ 0\ \ 5]^T$	-1.33×10^{-7}	-6.59×10^{-9}	9.41×10^{-9}	-3.42×10^{-8}	7.87×10^{-7}	4.70×10^{-5}
$[0\ \ 0\ \ 10]^T$	-2.76×10^{-7}	-1.37×10^{-8}	-7.16×10^{-9}	-6.85×10^{-8}	1.57×10^{-6}	9.41×10^{-5}

Table 2
Deformations of the compliant mechanisms in Example 1 when the force (parallel to z axis) is applied on the point $(r,\ 0,\ 0)$ mm.

$\boldsymbol{F}$ imposed on the point $(r,\ 0,\ 0)$mm (N)	Displacement along x axis (mm)		Displacement along y axis (mm)		Displacement along z axis (mm)	
	Parallel	Serial	Parallel	Serial	Parallel	Serial
$[0\ \ 0\ \ -10]^T$	−0.99	−0.9391	-1.48×10^{-2}	1.66×10^{-7}	3.42×10^{-2}	2.73×10^{-2}
$[0\ \ 0\ \ -5]^T$	−0.4968	−0.4846	-3.89×10^{-3}	6.93×10^{-8}	9.13×10^{-3}	7.21×10^{-3}
$[0\ \ 0\ \ 5]^T$	0.5048	0.5158	-4.32×10^{-3}	-8.10×10^{-8}	1.09×10^{-2}	8.45×10^{-3}
$[0\ \ 0\ \ 10]^T$	1.0233	1.0635	-1.83×10^{-2}	-1.63×10^{-7}	4.86×10^{-2}	3.56×10^{-2}

that of its serial counterpart as well as the ideal stiffness calculated theoretically. Here the mean margin of the stiffness errors is defined as

$$\lambda = \frac{\sum_{i=1}^{N} \frac{|\varepsilon_{ki}|}{k_{ideal}}}{N} \tag{84}$$

where ε_{ki} is the stiffness error of node i, N is the number of the nodes, and k_{ideal} is the ideal stiffness in theory.

As listed in Table 1, when the force (parallel to z axis) is applied on the point (0, 0, 0) mm, there are no deformations along x, y or z axis, which means the manipulator is stiff in this direction. Nevertheless, when the force is imposed on the point (r, 0, 0) mm, the deformation exists along x axis, see Table 2. In this situation, the direction of deformation is normal to that of the force.

6.2. Simulation of Example 2

In the simulation model of the compliant parallel mechanism, the stiffness of the three springs is equal to 10 N /mm. With Eq. (68), the stiffness of the two angular springs in the compliant serial mechanism is 2560 N · mm/rad, and the stiffness of the linear spring is 10 N/mm. As a compliant mechanism with planar 3 DOFs, the forces collinear with x axis and y axis as well as the torque about z axis are imposed on the point (0, 0, 0) mm to analyze the elastic behaviors. The deformations of the serial and parallel configurations in both theory and simulation are plotted in Fig. 16. Similar to Example 1, the elastic behaviors of the compliant serial mechanism approach to the ones calculated theoretically. For the compliant parallel mechanism, the translational stiffness along x axis and the angular stiffness about z axis are almost the same as that of its serial counterpart. By contrast, the translational stiffness along y axis gains gradually, as the force increases from −10 to 10 N. The mean margin of the stiffness errors along y axis is about 11.97%, when the force is in the range of [−10, 10] N. By contrast, the mean margin of the stiffness errors is 6.98%, when the force belongs to [−5, 5] N. Similar to Example 1, the stiffness approaches to that of its serial counterpart as well as the ideal stiffness in theory, when the amplitude of the force is close to zero.

6.3. Simulation of Example 3

In the simulation model of the compliant serial mechanism, the stiffness of the four angular springs is 2560 N · mm /rad. With Eq. (81), the stiffness parameters of the two linear springs in limbs 1 and 4 of the compliant parallel mechanism are equal to 9.92 N /mm, and the stiffness parameters of the two linear springs in limbs 2 and 3 are equal to 10 N/mm. As a compliant mechanism with spatial 4 DOFs, the forces collinear with x axis, y axis, and z axis are applied on the point (0, 0, 0) to analyze the elastic behaviors. The deformations of the serial and parallel configurations in both theory and simulation are depicted in Fig. 17. It is easily seen that the elastic behaviors of the compliant serial mechanism are close to that in theory. For the compliant parallel mechanism, the translational stiffness along z axis is almost the same as that of its serial counterpart, as shown in Fig. 17(c). However, as the force increases from −10 to 10 N, the translational stiffness along x axis decreases (see Fig. 17(a)), with the mean margin of stiffness errors about 12.33%. By contrast, the translational stiffness along y axis gains gradually (see Fig. 17(b)), with the mean margin of the stiffness errors about 12.93%. While the mean margins of the stiffness errors along x and y axes reduce to 3.66% and 3.75%, respectively, when the forces are bounded by −5 N to 5 N. When the forces along x axis and y axis are close to zero, the translational stiffness approaches to the ideal

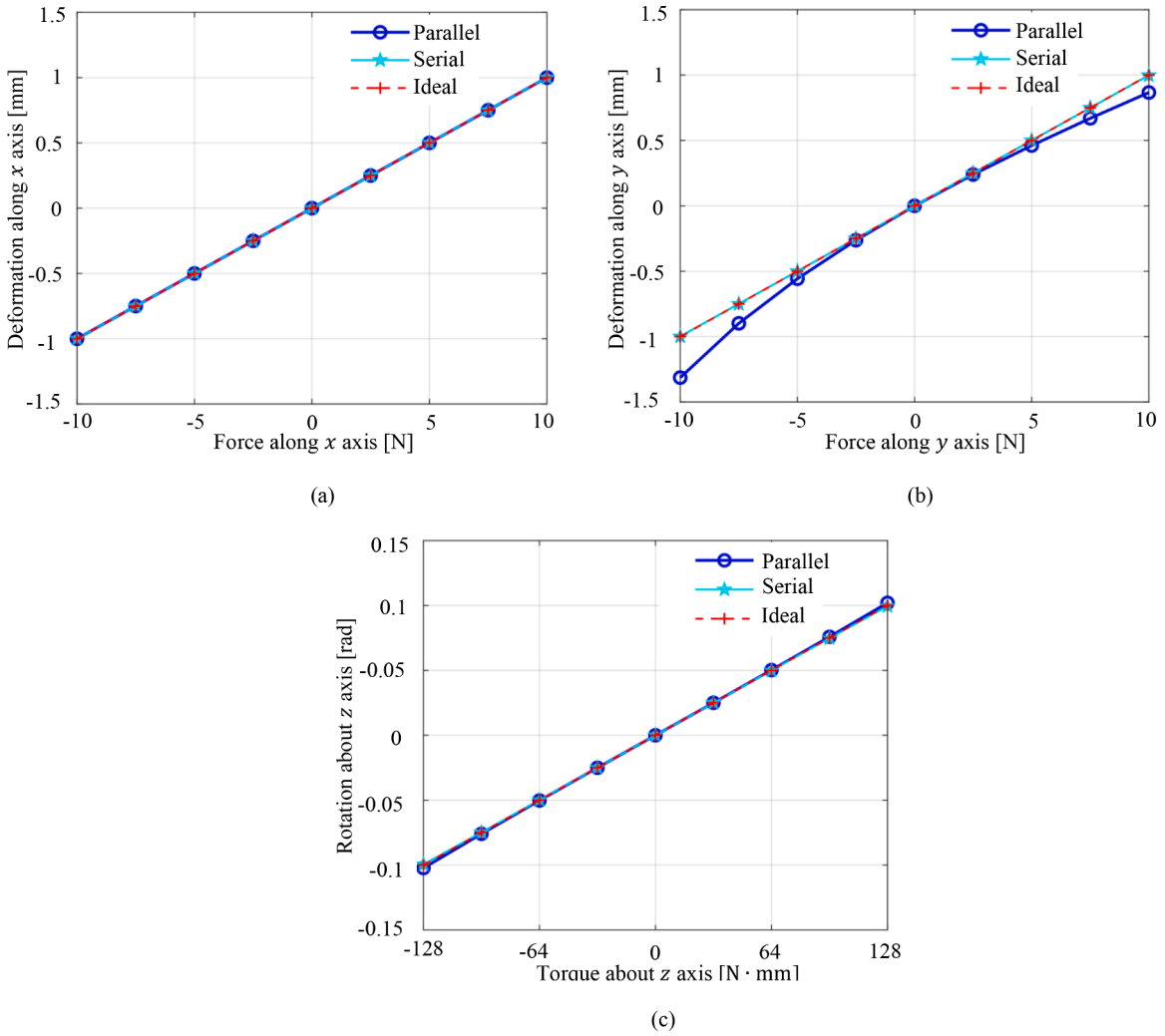

Fig. 16. Deformations of the compliant mechanisms in Example 1: (a, b) when the force is collinear with x axis and y axis, respectively, and (c) when the torque is about z axis.

stiffness in theory.

In summary, the elastic behaviors of the compliant serial mechanism are almost the same as the ideal ones calculated theoretically, while the stiffness/compliance of the compliant parallel mechanism may vary monotonically with respect to the force imposed on the platform in some directions. If the amplitude of the force is small, the stiffness/compliance of the parallel configuration is close to that of the theoretical model. The reason of the stiffness errors lies in that the displacement caused by the force leads to the change of the mechanical configuration. For parallel configurations, the change exists in all its limbs, while the change affect only a few joints of a serial configuration, not all. Thus the compliant parallel counterpart exhibits larger errors than the serial one.

7. Conclusion and future work

This paper introduced a geometrical interpretation of dualities of general compliant mechanisms using repelling screws, upon which both orthogonal and dual properties of the twist and wrench spaces were investigated and revealed. With the inclusion of constraints, the generalized interpretation of the mechanical geometries also laid a solid foundation for further analysis, such as errors, dexterity, and dynamics, etc. A novel approach for configuration transformation between compliant parallel and serial mechanisms was proposed, which makes a step forward from the mechanism-equivalent approach by modeling the relationships of the repelling screws and stiffness/compliance of compliant parallel and serial mechanisms, without the decomposition of the stiffness/compliance matrix. This paper extended the concept of dual elastic mechanisms to more general cases, including rank deficient compliances and constraints. With the proposed approach, the spatial elastic behaviors having constraints and/or rank deficiencies can be realized by either a compliant parallel or serial mechanism. Three representative examples were included to interpret the geometrical meaning of the stiffness/compliance and repelling screws. The equivalent kinematics and stiffness/compliance of the complaint parallel and serial

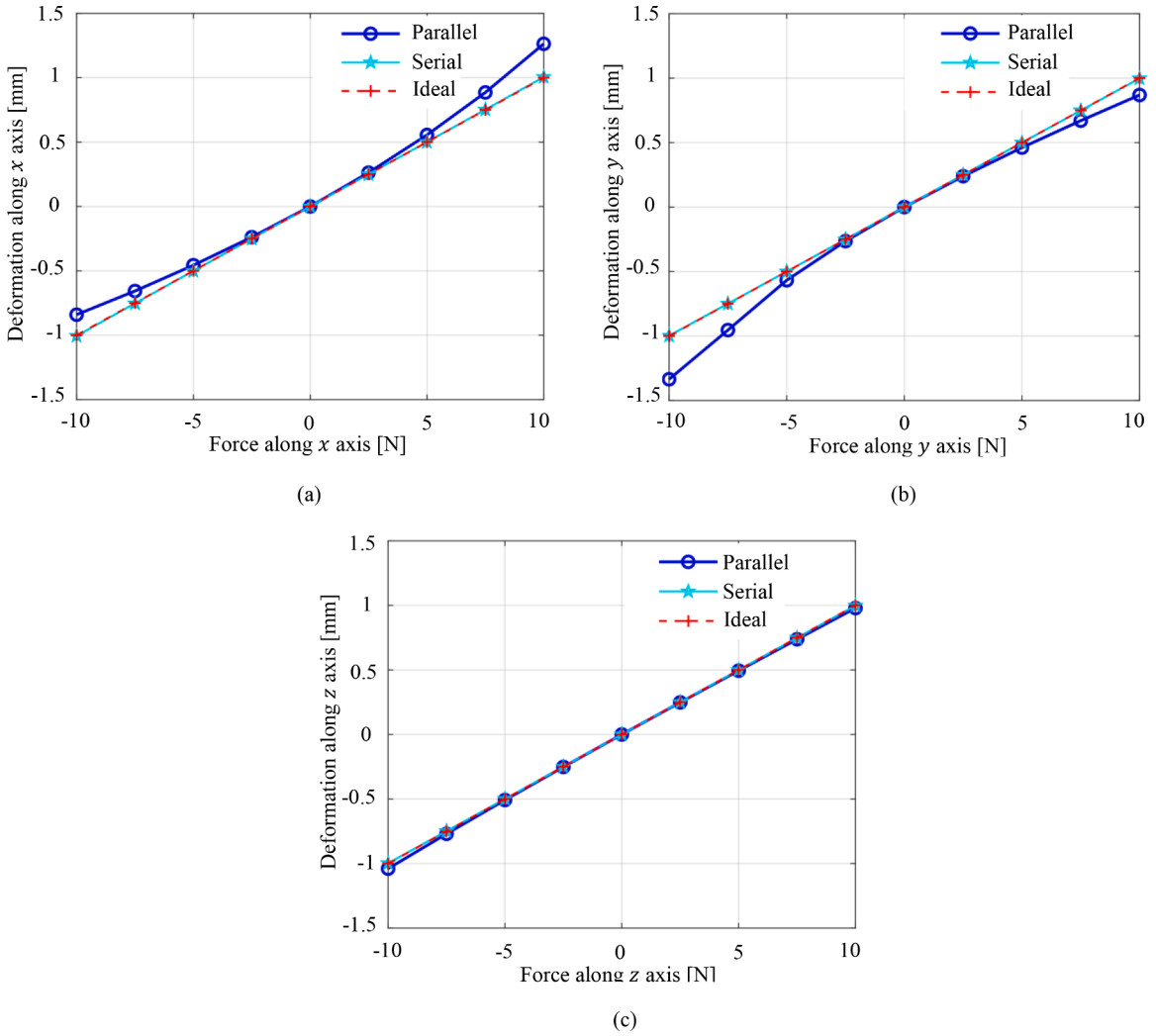

Fig. 17. Deformations of the compliant mechanisms in Example 3 when the force is collinear with (a) x axis, (b) y axis, and (c) z axis.

mechanisms were then discussed and illustrated. Moreover, two methods were proposed to adjust the target configuration so as to better suit the working conditions and installation limits. In terms of applications, one can use these methods to judiciously select a better mechanism geometry for a specified stiffness/compliance. The corresponding simulation models were established to verify the proposed approach, which demonstrated a good agreement between the geometrical and elastic properties of compliant parallel and serial mechanisms. The results also indicate that the proposed interpretation is extremely intuitive and provides a geometrical meaning for dualities of general compliant mechanisms. Hence, it can be potentially used in designing or discovering new compliant parallel or serial mechanisms.

In this paper, we mainly address the inner relations between the kinematics, statics, stiffness and compliance, as well as parallel and serial compliant systems. In real applications of compliant mechanisms, constraints may be designed on each limb, which can be equivalent to being imposed on the end effector. It will be explained in detail in our future work. Other aspects such as the geometrical and elastic properties of compliant mechanisms with redundant flexible/constraint limbs, and complicated hybrid flexible systems will be considered in future studies.

Declaration of Competing Interest

The authors declare that they have no known competing financial interests or personal relationships that could have appeared to influence the work reported in this paper.

References

[1] J.S. Dai, D.R. Kerr, A six-component contact force measurement device based on the Stewart platform, Proc. Inst. Mech. Eng. Part C J. Mech. Eng. 214 (2000) 687–697, https://doi.org/10.1243/0954406001523696.
[2] C. Yang, S. Geng, I. Walker, D.T. Branson, J. Liu, J.S. Dai, R. Kang, Geometric constraint-based modeling and analysis of a novel continuum robot with shape memory alloy initiated variable stiffness, Int. J. Rob. Res. 39 (2020) 1620–1634, https://doi.org/10.1177/0278364920913929.
[3] H. Dong, E. Asadi, C. Qiu, J. Dai, I.M. Chen, Geometric design optimization of an under-actuated tendon-driven robotic gripper, Robot. Comput. Integr. Manuf. 50 (2018) 80–89, https://doi.org/10.1016/j.rcim.2017.09.012.
[4] H. Dong, E. Asadi, C. Qiu, J. Dai, I.M. Chen, Grasp analysis and optimal design of robotic fingertip for two tendon-driven fingers, Mech. Mach. Theory 130 (2018) 447–462, https://doi.org/10.1016/j.mechmachtheory.2018.08.028.
[5] A.L. Orekhov, C.B. Black, J. Till, S. Chung, D.C. Rucker, Analysis and validation of a teleoperated surgical parallel continuum manipulator, IEEE Robot. Autom. Lett. 1 (2016) 828–835, https://doi.org/10.1109/LRA.2016.2525720.
[6] K.A. Jensen, C.P. Lusk, L.L. Howell, An XYZ micromanipulator with three translational degrees of freedom, Robotica 24 (2006) 305–314, https://doi.org/10.1017/S0263574705002134.
[7] A. Ataollahi, A.S. Fallah, L.D. Seneviratne, P. Dasgupta, K. Althoefer, Novel force sensing approach employing prismatic-tip optical fiber inside an orthoplanar spring structure, IEEE/ASME Trans. Mechatron. 19 (2014) 121–130, https://doi.org/10.1109/TMECH.2012.2222906.
[8] G. Hao, H. Li, A. Nayak, S. Caro, Design of a compliant gripper with multimode jaws, J. Mech. Robot. 10 (2018), 031005, https://doi.org/10.1115/1.4039498.
[9] L.L. Howell, S.P. Magleby, B.M. Olsen, Handbook of Compliant Mecahnisms, John Wiley & Sons, Ltd, 2013, https://doi.org/10.1002/9781118516485.
[10] C. Qiu, J.S. Dai, Analysis and Synthesis of Compliant Parallel Mechanisms-Screw Theory Approach, Springer International Publishing, 2021, https://doi.org/10.1007/978-3-030-48313-5.
[11] G. Chen, F. Ma, G. Hao, W. Zhu, Modeling large deflections of initially curved beams in compliant mechanisms using chained beam constraint model, J. Mech. Robot. 11 (2019), 011002, https://doi.org/10.1115/1.4041585.
[12] R.S. Ball, A Treatise on The Theory of Screws, Cambridge University Press, Cambridge, England, 1900.
[13] F.M. Dimentberg, The Screw Calculus and Its Applications in Mechanics, Foreign Technology Division, WP-AFB, 1968.
[14] J. Loncaric, Geometrical Analysis of Compliant Mechanisms in Robotics (Euclidean Group, Elastic Systems, Generalized Springs), Harvard University, 1985.
[15] S. Huang, J.M. Schimmels, Synthesis of planar compliances with mechanisms having six compliant components: geometric approach, J. Mech. Robot. 12 (2020), 031013, https://doi.org/10.1115/1.4045648.
[16] S. Huang, J.M. Schimmels, The eigenscrew decomposition of spatial stiffness matrices, IEEE Trans. Robot. Autom. 16 (2000) 146–156, https://doi.org/10.1109/70.843170.
[17] S. Huang, J.M. Schimmels, The bounds and realization of spatial stiffnesses achieved with simple springs connected in parallel, IEEE Trans. Robot. Autom. 14 (1998) 466–475, https://doi.org/10.1109/70.678455.
[18] S. Huang, J.M. Schimmels, Geometric construction-based realization of spatial elastic behaviors in parallel and serial manipulators, IEEE Trans. Robot. 34 (2018) 764–780, https://doi.org/10.1109/TRO.2018.2805315.
[19] S. Huang, J.M. Schimmels, Synthesis of point planar elastic behaviors using three-joint serial mechanisms of specified construction, J. Mech. Robot. 9 (2017), 011005, https://doi.org/10.1115/1.4035189.
[20] S. Huang, J.M. Schimmels, Geometric construction-based realization of planar elastic behaviors with parallel and serial manipulators, J. Mech. Robot. 9 (2017) 1–10, https://doi.org/10.1115/1.4037019.
[21] M.B. Hong, Y.J. Choi, Screw system approach to physical realization of stiffness matrix with arbitrary rank, J. Mech. Robot. 1 (2009) 1–8, https://doi.org/10.1115/1.3046146.
[22] G. Chen, H. Wang, Z. Lin, X. Lai, The principal axes decomposition of spatial stiffness matrices, IEEE Trans. Robot. 31 (2015) 191–207, https://doi.org/10.1109/TRO.2015.2389415.
[23] H. Dong, C. Qiu, D.K. Prasad, Y. Pan, J. Dai, I.M. Chen, Enabling grasp action: generalized quality evaluation of grasp stability via contact stiffness from contact mechanics insight, Mech. Mach. Theory. 134 (2019) 625–644, https://doi.org/10.1016/j.mechmachtheory.2019.01.019.
[24] J.S. Dai, X. Ding, Compliance analysis of a three-legged rigidly-connected platform device, J. Mech. Des. Trans. ASME 128 (2006) 755–764, https://doi.org/10.1115/1.2202141.
[25] N. Simaan, M. Shoham, Stiffness synthesis of a variable geometry six-degrees-of-freedom double planar parallel robot, Int. J. Rob. Res. 22 (2004) 757–775, https://doi.org/10.1177/027836403128965330.
[26] X. Ding, J.S. Dai, Characteristic equation-based dynamics analysis of vibratory bowl feeders with three spatial compliant legs, IEEE Trans. Autom. Sci. Eng. 5 (2008) 164–175, https://doi.org/10.1109/TASE.2007.910301.
[27] K. Wu, G. Hao, Design and nonlinear modeling of a novel planar compliant parallelogram mechanism with general tensural-compresural beams, Mech. Mach. Theory 152 (2020) 1–23, https://doi.org/10.1016/j.mechmachtheory.2020.103950.
[28] S. Awtar, J. Ustick, S. Sen, An XYZ parallel-kinematic flexure mechanism with geometrically decoupled degrees of freedom, J. Mech. Robot. 5 (2013), 015001, https://doi.org/10.1115/1.4007768.
[29] J.S. Dai, J. Rees, Interrelationship between screw systems and corresponding reciprocal systems and applications, Mech. Mach. Theory 36 (2001) 633–651, https://doi.org/10.1016/S0094-114X(01)00004-0.
[30] D. Blanding, Exact Constraint: Machine Design Using Kinematic Principles, ASME Press, 1999, https://doi.org/10.1115/1.800857.
[31] J.B. Hopkins, M.L. Culpepper, Synthesis of multi-degree of freedom, parallel flexure system concepts via freedom and constraint topology (FACT). Part II: practice, Precis. Eng. 34 (2010) 271–278, https://doi.org/10.1016/j.precisioneng.2009.06.007.
[32] J.B. Hopkins, M.L. Culpepper, Synthesis of multi-degree of freedom, parallel flexure system concepts via freedom and constraint topology (FACT)-part I : principles, Precis. Eng. 34 (2010) 259–270, https://doi.org/10.1016/j.precisioneng.2009.06.008.
[33] J.B. Hopkins, M.L. Culpepper, Synthesis of precision serial flexure systems using freedom and constraint topologies (FACT), Precis. Eng. 35 (2011) 638–649, https://doi.org/10.1016/j.precisioneng.2011.04.006.
[34] J.J. Yu, S.Z. Li, X. Pei, H.J. Su, J.B. Hopkins, M.L. Culpepper, Type synthesis principle and practice of flexure systems in the framework of screw theory part I: general methodology, Proc. ASME Des. Eng. Tech. Conf. 2 (2010) 543–552, https://doi.org/10.1115/DETC2010-28783.
[35] J.J. Yu, X. Pei, S.Z. Li, H.J. Su, J.B. Hopkins, M.L. Culpepper, Type synthesis principle and practice of flexure systems in the framework of screw theory Part II: numerations and synthesis of complex flexible joints, Proc. ASME Des. Eng. Tech. Conf. 2 (2010) 553–561, https://doi.org/10.1115/DETC2010-28794.
[36] H.J. Su, Mobility analysis of flexure mechanisms via screw algebra, J. Mech. Robot. (2011) 3, https://doi.org/10.1115/1.4004910.
[37] H.J. Su, D.V. Dorozhkin, J.M. Vance, A screw theory approach for the conceptual design of flexible joints for compliant mechanisms, J. Mech. Robot. 1 (2009) 1–8, https://doi.org/10.1115/1.3211024.
[38] H.J. Su, H. Tari, Realizing orthogonal motions with wire flexures connected in parallel, J. Mech. Des. Trans. ASME 132 (2010) 1–7, https://doi.org/10.1115/1.4002837.
[39] H.J. Su, H. Tari, On line screw systems and their application to flexure synthesis, J. Mech. Robot. 3 (2011) 1–7, https://doi.org/10.1115/1.4003078.
[40] H.J. Su, H. Shi, J. Yu, A symbolic formulation for analytical compliance analysis and synthesis of flexure mechanisms, J. Mech. Des. Trans. ASME (2012) 134, https://doi.org/10.1115/1.4006441.
[41] J.B. Hopkins, M.L. Culpepper, A screw theory basis for quantitative and graphical design tools that define layout of actuators to minimize parasitic errors in parallel flexure systems, Precis. Eng. 34 (2010) 767–776, https://doi.org/10.1016/j.precisioneng.2010.05.004.
[42] J. Yu, S. Li, C. Qiu, An analytical approach for synthesizing line actuation spaces of parallel flexure mechanisms, J. Mech. Des. Trans. ASME 135 (2013) 1–5, https://doi.org/10.1115/1.4025289.
[43] S.M. Girvin, Duality in perspective, Science 274 (80) (1996) 524–525, https://doi.org/10.1126/science.274.5287.524.

[44] K.J. Waldron, K.H. Hunt, Series-parallel dualities in actively coordinated mechanisms, Int. J. Rob. Res. 10 (1991) 473–480, https://doi.org/10.1177/027836499101000503.
[45] C.L. Collins, G.L. Long, On the duality of twist/wrench distributions in serial and parallel chain robot manipulators, in: Proceedings of the IEEE International Conference on Robotics and Automation, 1995, pp. 526–531, https://doi.org/10.1109/ROBOT.1995.525337.
[46] F. Gosselin, J.P. Lallemand, A new insight into the duality between serial and parallel non-redundant and redundant manipulators, Robotica 19 (2001) 365–370, https://doi.org/10.1017/S0263574701003332.
[47] J. Duffy, Statics and Kinematics With Applications to Robotics, Cambridge University Press, Cambridge, England, 1996, https://doi.org/10.1017/cbo9780511530173.
[48] J.K. Davidson, K.H. Hunt, Robots and Screw Theory: Applications of Kinematics and Statics to Robotics, Oxford University Press, New York, 2004.
[49] O. Shai, G.R. Pennock, Extension of graph theory to the duality between static systems and mechanisms, J. Mech. Des. Trans. ASME 128 (2006) 179–191, https://doi.org/10.1115/1.2120827.
[50] O. Shai, G.R. Pennock, A study of the duality between planar kinematics and statics, J. Mech. Des. Trans. ASME 128 (2006) 587–598, https://doi.org/10.1115/1.2181600.
[51] T. Huang, H.T. Liu, D.G. Chetwynd, Generalized Jacobian analysis of lower mobility manipulators, Mech. Mach. Theory 46 (2011) 831–844, https://doi.org/10.1016/j.mechmachtheory.2011.01.009.
[52] S. Huang, J.M. Schimmels, The duality in spatial stiffness and compliance as realized in parallel and serial elastic mechanisms, J. Dyn. Syst. Meas. Control. Trans. ASME 124 (2002) 76–84, https://doi.org/10.1115/1.1434273.
[53] M. Ohwovoriole, B. Roth, An extension of screw theory, J. Mech. Des. 103 (1981) 725–735, https://doi.org/10.1115/1.3254979.
[54] C. Qiu, K. Zhang, J.S. Dai, Repelling-screw based force analysis of origami mechanisms, J. Mech. Robot. 8 (2016), 031001, https://doi.org/10.1115/1.4031458.
[55] C.L.C. Gregory, L. Long, On the duality of twist/wrench distributions in serial and parallel chain robot manipulators, in: Proceedings of the IEEE International Conference on Robotics and Automation, 1995, pp. 526–531, https://doi.org/10.1109/ROBOT.1995.525337.
[56] J.S. Dai, An historical review of the theoretical development of rigid body displacements from Rodrigues parameters to the finite twist, Mech. Mach. Theory 41 (2006) 41–52, https://doi.org/10.1016/j.mechmachtheory.2005.04.004.
[57] J. Plücker, On a new geometry of space, Proc. R. Soc. Lond. 14 (1865) 53–58, https://doi.org/10.1098/rspl.1865.0014.
[58] H. Lipkin, J. Duffy, The elliptic polarity of screws, J. Mech. Des. Trans. ASME 107 (1985) 377–386, https://doi.org/10.1115/1.3260725.
[59] L. Hogben, Handbook of Linear Algebra, 2nd ed., Chapman and Hall/CRC, 2013 https://doi.org/10.1201/b16113.
[60] C.D. Meyer, Matrix Analysis and Linear Algebra, SIAM, Philadelphia, 2000.
[61] K. Sugimotot, J. Duffy, Application of linear algebra to screw systems, Mech. Mech. Theory 17 (1982) 73–83, https://doi.org/10.1016/0094-114X(82)90025-8.
[62] J.S. Dai, J.R. Jones, A linear algebraic procedure in obtaining reciprocal screw systems, J. Robotic Syst. 20 (2003) 401–412, https://doi.org/10.1002/rob.10094.
[63] J.S. Dai, J.R. Jones, Null-space construction using cofactors from a screw-algebra, Proc. R. Soc. A 458 (2002) 1845–1866, https://doi.org/10.1098/rspa.2001.0949.
[64] L.W. Tsai, Robot Analysis: The Mechanics of Serial and Parallel Manipulators, John Wiley & Sons, New York, 1999.
[65] J.S. Dai, Geometrical Foundations and Screw Algebra For Mechanisms and Robotics, Higher Education Press, Beijing, 2014.
[66] J.S. Dai, Z. Huang, H. Lipkin, Mobility of overconstrained parallel mechanisms, J. Mech. Des. Trans. ASME 128 (2006) 220–229, https://doi.org/10.1115/1.1901708.
[67] K.B. Petersen, M.S. Pedersen, The Matrix Cookbook, Technical University of Denmark, 2012.
[68] B. Yi, G.B. Chung, H.Y. Na, W.K. Kim, I.H. Suh, Design and experiment of a 3-DOF parallel micromechanism utilizing flexure hinges, IEEE Trans. Robot. 19 (2003) 604–612, https://doi.org/10.1109/TRA.2003.814511.
[69] C. Qiu, J.S. Dai, Constraint stiffness construction and decomposition of a SPS orthogonal parallel mechanism, in: Proceedings of the 39th Mechanisms and Robotics Conference, 2015, pp. 1–9.
[70] C. Qiu, P. Qi, H. Liu, K. Althoefer, J.S. Dai, Six-dimensional compliance analysis and validation of orthoplanar springs, J. Mech. Des. 138 (2016), 042301, https://doi.org/10.1115/1.4032580.
[71] G. Hao, H. Li, Design of 3-legged XYZ compliant parallel manipulators with minimised parasitic rotations, Robotica 33 (2015) 787–806, https://doi.org/10.1017/S0263574714000575.
[72] G. Chen, Y. Ding, X. Zhu, P. Liu, H. Ding, Design and modeling of a compliant tip-tilt-piston micropositioning stage with a large rotation range, Proc. Inst. Mech. Eng. Part C J. Mech. Eng. Sci. 233 (2019) 2001–2014, https://doi.org/10.1177/0954406218781401.
[73] M.T. Pham, S.H. Yeo, T.J. Teo, P. Wang, M.L.S. Nai, Design and optimization of a three degrees-of-freedom spatial motion compliant parallel mechanism with fully decoupled motion characteristics, J. Mech. Robot. 11 (2019), 051010, https://doi.org/10.1115/1.4043925.
[74] C. Qiu, K. Zhang, J.S. Dai, Constraint-based design and analysis of a compliant parallel mechanism using SMA-spring actuators, in: Proceedings of the International Design Engineering Technical Conferences and Computers and Information in Engineering Conference, Volume 5A: 38th Mechanisms and Robotics Conference, ASME, 2014 p. V05AT08A035.
[75] J.M. Schimmels, S. Huang, Spatial parallel compliant mechanism, US Patent US006021579A, 2000.
[76] R. Wang, X. Zhou, Z. Zhu, Q. Liu, Compliant linear-rotation motion transduction element based on novel spatial helical flexure hinge, Mech. Mach. Theory 92 (2015) 330–337, https://doi.org/10.1016/j.mechmachtheory.2015.06.005.